



National Library  
of Canada

Bibliothèque nationale  
du Canada

Canadian Theses Service / Service des thèses canadiennes

Ottawa, Canada  
K1A 0N4

## NOTICE

The quality of this microform is heavily dependent upon the quality of the original thesis submitted for microfilming. Every effort has been made to ensure the highest quality of reproduction possible.

If pages are missing, contact the university which granted the degree.

Some pages may have indistinct print, especially if the original pages were typed with a poor typewriter ribbon or if the university sent us an inferior photocopy.

Previously copyrighted materials (journal articles, published tests, etc.) are not filmed.

Reproduction in full or in part of this microform is governed by the Canadian Copyright Act, R.S.C. 1970, c. C.30.

## AVIS

La qualité de cette microforme dépend grandement de la qualité de la thèse soumise au microfilmage. Tous les efforts ont été faits pour assurer une qualité supérieure de reproduction.

Si manque des pages, veuillez vous adresser à l'université qui a conféré le grade.

La qualité d'impression de certaines pages peut être affectée, surtout si les pages originales ont été tapées à l'aide d'un ruban de mauvaise qualité ou si la photocopie envoyée est de qualité inférieure.

Les documents qui font déjà l'objet d'un droit d'auteur (articles de revue, tests publiés, etc.) ne sont pas microfilmés.

La reproduction, même partielle, de cette microforme est soumise à la Loi canadienne sur le droit d'auteur, 1970, c. C.30.

THE UNIVERSITY OF ALBERTA

Fluid Inclusion and  $\delta^{18}\text{O}$  Study of the Precious Metal Bearing Veins of the Wheaton River

District, Yukon

by



Paul Douglas Rucker

A THESIS

SUBMITTED TO THE FACULTY OF GRADUATE STUDIES AND RESEARCH

IN PARTIAL FULFILLMENT OF THE REQUIREMENTS FOR THE DEGREE

OF MASTER OF SCIENCE

DEPARTMENT OF GEOLOGY

EDMONTON, ALBERTA

Spring, 1988

Permission has been granted to the National Library of Canada to microfilm this thesis and to lend or sell copies of the film.

The author (copyright owner) has reserved other publication rights, and neither the thesis nor extensive extracts from it may be printed or otherwise reproduced without his/her written permission.

L'autorisation a été accordée à la Bibliothèque nationale du Canada de microfilmer cette thèse et de prêter ou de vendre des exemplaires du film.

L'auteur (titulaire du droit d'auteur) se réserve les autres droits de publication; ni la thèse ni de longs extraits de celle-ci ne doivent être imprimés ou autrement reproduits sans son autorisation écrite.

ISBN 0 315-42879-1

THE UNIVERSITY OF ALBERTA

RELEASE FORM

NAME OF AUTHOR Paul Douglas Rucker  
TITLE OF THESIS Fluid Inclusion and  $\delta^{18}\text{O}$  Study of the Precious Metal-Bearing Veins  
of the Wheaton River District, Yukon.  
DEGREE FOR WHICH THESIS WAS PRESENTED MASTER OF SCIENCE  
YEAR THIS DEGREE GRANTED Spring, 1988

Permission is hereby granted to THE UNIVERSITY OF ALBERTA LIBRARY  
to reproduce single copies of this thesis and to lend or sell such copies for private,  
scholarly or scientific research purposes only.

The author reserves other publication rights, and neither the thesis nor extensive  
extracts from it may be printed or otherwise reproduced without the author's written  
permission.

(SIGNED)

*Paul D. Rucker*

PERMANENT ADDRESS:

*Rt. 1, Box 226*

*Webbville, KY 41180*

*U.S.A.*

DATED *Nov 2* 1987

THE UNIVERSITY OF ALBERTA  
FACULTY OF GRADUATE STUDIES AND RESEARCH

The undersigned certify that they have read, and recommend to the Faculty of Graduate Studies and Research, for acceptance, a thesis entitled Fluid Inclusion and  $\delta^{18}O$  Study of the Precious Metal-Bearing Veins of the Wheaton River District, Yukon, submitted by Paul Douglas Rucker in partial fulfilment of the requirements for the degree of MASTER OF SCIENCE.

*[Handwritten signature]*  
.....

Supervisor

*H. Boadgaard*  
.....

*[Handwritten signature]*  
.....

*[Handwritten signature]*  
.....

Date *2 Dec 1981*  
.....

Dedication

To my family

## Abstract

The Wheaton River district encompasses sulfide-bearing quartz veins of three basic types: stibnite-bearing, galena-bearing, and arsenopyrite-bearing. The veins are distributed over a wide area in southwestern Yukon and are hosted in several different rock types in a geologically complex area. Regional geology is dominated by the Coast Plutonic Complex, the Intermontane Belt, and Yukon Crystalline Terrane. The veins were deposited in minor faults and fractures whose walls show variable degrees of alteration. Temporal relationships are unclear due to a lack of datable vein material and the absence of cross-cutting relationships among the veins.

All vein types exhibit relatively simple depositional sequences, usually consisting of one or, at most, two periods of sulfide mineralization. During any depositional episode, the sulfides were always deposited sequentially as evidenced by replacement and infilling textures.

Fluid inclusions occur as three broad types: I. H<sub>2</sub>O-NaCl, II. H<sub>2</sub>O-CO<sub>2</sub>-NaCl, and III. CO<sub>2</sub>. Fluid inclusions in stibnite-bearing veins give homogenization temperatures of  $\approx 200^{\circ}\text{C}$ , while those in galena-bearing veins give homogenization temperatures of  $225\text{--}311^{\circ}\text{C}$ . Salinities for both types of veins average around 4.0 wt.% eq. NaCl. CO<sub>2</sub> effervescence may have occurred in the stibnite-bearing veins as evidenced by adjacent primary CO<sub>2</sub> and H<sub>2</sub>O-NaCl inclusions. Inclusions in one galena-bearing vein exhibit critical behavior suggesting near solvus conditions. Effervescence of CO<sub>2</sub> in these two types of veins may mean that effervescence was the mechanism which initiated sulfide precipitation. Pressure estimates based on fluid inclusion data are in the range 500 to 1500 bars suggesting possible circulation depths of over 5km.

Oxygen isotope analyses give values which are enriched relative to SMOW. When these values are combined with fluid inclusion, homogenization temperature data, parent fluid <sup>18</sup>O values of 2.2 to 5.7‰ are obtained for most showings. Fluid  $\delta^{18}\text{O}$  values for two showings of galena-bearing veins fall below this range. A few values mostly derived from chalcedony or fine-grained quartz are highly depleted relative to the principal veins. These three groups of  $\delta^{18}\text{O}$  data can be explained by several mechanisms, but  $\delta\text{D}$  data are required to give a better

indication as to which mechanism is most plausible.

When all evidence (mineralogy, petrology, fluid inclusion, and isotopes) is considered, only a system (or systems) of some complexity could account for such variable data. As no  $\delta D$  data are available, it is possible to speculate that any of the three principal types of natural waters (magmatic, metamorphic and meteoric) served as the primary source of the parent fluids for any of the sulfide-bearing veins. Various mechanisms, such as mixing of fluids, fluid immiscibility and later overprinting, are possible explanations for the  $\delta^{18}O$  content of the parent fluids.



## Acknowledgements

During the course of my studies at the University of Alberta, I have met numerous people who have given me support and encouragement for which I will always be grateful. First, I would like to thank my supervisor, Bruce Nesbitt. He initiated this project and provided support of all kinds throughout its course. He also showed great patience and understanding when things were going slowly.

Dr. Karlis Muchlenbachs' analyses of oxygen isotope samples are greatly appreciated. I would also like to thank the other members of my committee, Dr. H. Baadsgaard and Dr. Jerry Whiting, for their comments and suggestions.

Funding and field support were provided by D.I.A.N.D. in Whitehorse. The assistance of Jim Morin and his staff at D.I.A.N.D. was essential to the completion of this study.

I wish to express my gratitude to all the members of the Department of Geology (Faculty, staff, graduate students and undergraduates) for the assistance and friendship they provided during my stay. I, especially, would like to thank the other members of the Economic Geology group, past and present, whose ideas and suggestions were invaluable.

Special thanks are due to the close friends I made in Edmonton who made things a little more sane while I was there.

Thanks to Pierre, roommate, officemate, and friend. Good luck.

Thanks to Gwen, for everything.

## Table of Contents

Chapter	Page
I. INTRODUCTION .....	1
A. Location and Access .....	1
B. Physiography .....	1
C. Exploration History .....	2
D. Purpose of Study .....	4
II. REGIONAL GEOLOGY .....	5
A. Tectonic Assemblage .....	5
B. Coast Plutonic Complex .....	5
C. Intermontane Belt .....	5
Whitehorse Trough .....	5
Yukon Crystalline Terrane .....	8
D. Volcanic Units .....	10
Skukum Group .....	10
Mesozoic Volcanics .....	10
E. Regional Structural Trends .....	12
III. MINERAL OCCURRENCES .....	13
A. Introduction .....	13
B. Stibnite-bearing Veins .....	13
Yukon Antimony .....	13
Porter Claims .....	15
Goddell's Claims .....	16
C. Galena-bearing Veins .....	16
Mt. Anderson .....	16
Mt. Stevens .....	17
Tally-Ho Hill .....	17
Gold Hill .....	18

Mt. Reid .....	18
D. Arsenopyrite-bearing Veins .....	19
IV. MINERALOGY AND PETROLOGY .....	20
A. Introduction .....	20
B. Stibnite-bearing Veins .....	20
Host-rock Petrology .....	20
Vein Mineralogy and Petrology .....	22
Paragenesis .....	23
C. Galena-bearing Veins .....	28
Host-rock Petrology .....	28
Vein Mineralogy and Petrology .....	30
Paragenesis .....	34
D. Arsenopyrite-bearing Veins .....	36
Host-rock Petrology .....	36
Vein Mineralogy and Petrology .....	36
Paragenesis .....	39
E. Discussion .....	41
V. FLUID INCLUSION STUDY .....	43
A. Introduction .....	43
B. Inclusion Petrography .....	43
C. Techniques and Apparatus .....	44
D. Low Temperature Measurements .....	48
E. High Temperature Measurements .....	58
F. Discussion of Results .....	58
Stibnite-bearing Veins .....	58
Galena-bearing Veins .....	59
Other veins .....	60

VI. OXYGEN ISOTOPE STUDY .....	62
A. Introduction .....	62
B. Techniques .....	62
C. Results of Analyses .....	63
D. Fluid Calculations .....	65
E. Discussion of Results .....	66
Normal Fluids .....	66
Depleted Fluids .....	66
Present Day Meteoric Water .....	68
VII. DISCUSSION AND CONCLUSIONS .....	71
A. Introduction .....	71
B. Models for Vein Deposition .....	73
Galena-bearing Veins .....	73
Low <sup>18</sup> O Galena-bearing Veins .....	75
Stibnite-bearing veins .....	77
REFERENCES .....	80
Appendix I .....	94
Appendix II .....	95

## List of Tables

Table		Page
V.1	Average values derived from fluid inclusion data, listed by locality (See Appendix I for list of abbreviations) .....	49
VI	Results of oxygen isotope analyses (See Appendix I for list of abbreviations) .....	64

## List of Figures

Figure	Page
II-1 Tectonic assemblage map of southwestern Yukon and northwestern British Columbia and location map of study area. Modified after Moser et al., 1979 and Tempelman-Kluit, 1981.	6
II-2 Regional geology of southwestern Yukon showing locations of volcanic centers. Modified after Carnes, 1912 and Wheeler, 1961.	9
II-3 Geology of the Wheaton River Valley with locations indicated of principal peaks. Modified after Wheeler, 1961.	11
III-4 Map showing locations of the principal mineral occurrences in the Wheaton River valley.	14
IV-7 Block of paragenetic sequences of the strubbe-bearing veins.	24
IV-9 Block of paragenetic sequences of two palena-bearing veins.	38
IV-10 Block of paragenetic sequence of the arsenopyrite-bearing veins.	40
V-5 Fluid inclusion ice-brine melting temperatures.	50
V-9 Fluid inclusion CO <sub>2</sub> clathrate melting temperatures.	51
V-10 Salinities derived from ImIce and ImClath measurements.	52
V-11 Fluid inclusion CO <sub>2</sub> melting temperatures.	53
V-12 Fluid inclusion CO <sub>2</sub> homogenization temperatures.	54
V-13 Fluid inclusion homogenization temperatures.	55
VI-14 $\delta^{18}O$ versus $\delta D$ plot showing data from this study in relation to other deposits. Upper $\delta D$ limit from Magaritz and Taylor, 1976, lower from Walton, 1987.	70
VII-15 Map showing the distribution of isotopic and fluid inclusion data in the study area.	72

## List of Plates

Plate		Page
IV 1	Radial growth pattern of second generation quartz overgrowth on first generation quartz core. Field of view is 1.5mm	25
IV 2	Stibnite needles outlining growth zones in quartz from the Potter adit. Field of view is 1.5mm	26
IV 3	Fine grained stibnite embracing quartz grains from Goddell's Claims. Field of view is 1.5mm	27
IV 4	Photomicrograph illustrating typical alteration in granitic rocks from Carbon Hill. Field of view is 1.5mm	29
IV 5	Granitic rock from Mt. Anderson exhibiting similar alteration as that from Carbon Hill. Field of view is 1.5mm	29
IV 6	Heavily corroded galena (white) from Mt. Stevens showing . . . . . Field of view is 1.5mm	33
IV 7	Arsenopyrite (light gray) from Idaho Hill with galena (darker gray) filling cavities. Field of view is 1.5mm	38
V 8	Type I inclusion from Mt. Anderson. Field of view is 0.75mm	45
V 9	Type II inclusion from Gold Hill, bubble is CO <sub>2</sub> . Field of view is 0.75mm	46
V 10	Type III inclusion from Yukon Ammony adit, Carbon Hill. Field of view is 0.75mm	47

## I. INTRODUCTION

### A. Location and Access

The Wheaton River district is situated in southcentral Yukon Territory approximately 50 km south of Whitehorse, (N.T.S. Map Sheet 105 D). The district encompasses an area roughly 26 km by 16 km, from the "Big Bend" of the Wheaton River along its valley southwestward toward its headwaters. The area is bounded by a rectangle defined by the 134° 59' W and 135° 30' W lines of longitude and the 60° 08' N and 60° 23' N lines of latitude.

In 1985, access was quite good due to improvements made to Annie Lake Road and its extension into the Wheaton Valley. This is a wide gravel road that intersects Carcross Road approximately 33 km south of Whitehorse. The improvements were made to facilitate travel to and from the Mt. Skukum gold property, which has since gone into production. By mid-summer the condition of the road was such that two-wheel drive vehicles could traverse its length. A four-wheel drive vehicle was necessary to reach individual properties. Over the course of the summer various companies working in the valley opened roads, if no passable road already existed, to all of the principal mineral showings in the area so that it was possible to get to all of these properties by vehicle. In some cases this meant being able to drive right to the showing, in most instances however a hike of some distance was required.

### B. Physiography

The Wheaton District is situated near the junction of two of the principal physiographic regions of the northern Cordillera. These regions are the Yukon Plateau and the Coast Ranges. The plateau is a mature erosion surface of probable Miocene age exhibiting little relief (Tempelman-Kluit, 1980). The rugged Coast Ranges took shape during the differential uplift of various parts of this erosion surface in late Miocene or Pliocene and the subsequent rapid erosion of the rising landscape. In the Wheaton, ~~area~~ the Plateau's erosion surface is abundantly evident in the gently rolling upland terrain, which forms the summits of all the major peaks of the valley, except Mt. Skukum. The jagged outline of the Coast Ranges



is readily visible immediately southwest of Carbon Hill

The Wheaton River Valley itself and its major tributary creek valleys have been deeply incised into the ancient erosion surface. Average relief from the valley bottom to the upland surface is approximately 690m. The master valley and tributary valleys all exhibit U shaped cross sections as a result of Pleistocene glaciation. Minor streams have cut deep V shaped channels in a few places, e.g. Carbon Hill, Mt. Folle and Idaho Hill, and in some cases have cut down into bedrock. Talus cover on the mountain slopes is quite extensive which means that outcrop, other than that in the above mentioned stream channels, is limited to that area between the upper level of rubble accumulation and the mountain summits. The upland surface is extensively weathered and covered somewhat variably by vegetation thus precluding the likelihood of finding fresh exposures on the mountain tops.

### C. Exploration History

Frank Corwin and Thomas Rickman staked the first claims in the valley in 1893, concentrating mainly on Idaho Hill, Carbon Hill and Chieftain Hill. Although their discoveries sparked great interest in the region, this led to little activity because both men died before either could return to the valley or reveal the claim locations. Not until a staking rush caused by the discovery of native gold in a vein on Gold Hill in the summer of 1906 was there a real resurgence of exploration in the valley. By the end of that summer all of the principal mineral showings of the valley had been located or, as in the case of some, relocated. It was this rush that led the Geological Survey of Canada to send D. D. Cairnes (1912 and 1916) to map the Wheaton District and determine its geology. Since that time, prospecting and evaluation activities, using increasingly modern methods as they became available, have been carried out sporadically.

Only two properties are known to have shipped ore prior to 1985, namely the Union Mines claims on Idaho Hill and the Tally-Ho claims on Tally-Ho Hill. In each case the ores were a limited number of hand-picked loads. The Union Mines ores were shipped because of their high silver values and the Tally-Ho ores because of their gold content. The lack of

production in the valley as a whole was no doubt due in large part to the extreme variability of metal values within the veins, which is the rule in the district. While spectacular assays of up to 4688.5g/T Ag and 67.5g/T Au are known, they invariably come from ore shoots which are very limited in extent within the veins (Cockfield and Bell, 1944).

A second period of relatively intense exploration activity occurred in the mid-1960's and continued into the early 1970's. At that time, Silver Pack Mines on Tally-Ho Hill, Yukon Antimony Corporation on Carbon Hill and Cominco Ltd. on Idaho Hill carried out extensive evaluation programs. Predictably, interest waned when these programs failed to delineate new deposits or sufficient reserves to warrant mining. The discovery of a totally new and unsuspected gold showing on Mt. Skukum by AGIP Canada in 1980 again drew attention to the area. The showing, which is apparently epithermal in nature, consists of a number of quartz-carbonate veins hosted in the Skukum Volcanic Complex. The largest of these veins is of particular interest because of the presence of microscopic particles of electrum disseminated throughout the vein with little or no associated sulfides. The absence of sulfides was generally believed to be quite rare in epithermal deposits (Berger and Eimon, 1982; Hayba *et al.*, 1985); however, this may have been an example of circular reasoning, i.e. only sulfide-bearing veins produced gold, therefore only sulfide-bearing veins were extensively explored for gold. If this was the case, it seems probable that many potentially significant deposits were ignored as ostensibly barren veins were discounted as being likely exploration targets. The Skukum deposit went into production in 1986 with proven reserves in the 'Main Zone' of 148,980 tonnes at grades of 24.98 g/T Au and 20.5 g/T Ag (McDonald, 1986). The presence of a probable gold producer in the vicinity touched off a flurry of activity that continues to the present. In the summer of 1985, upwards of fourteen companies were working or had at least staked claims in the area. As a result of this activity it appears that the Mt. Reid property controlled by Omni Resources may well begin producing gold in the near future.

#### D. Purpose of Study

Despite the long history of the Wheaton River District, no truly regional study of the various veins was made other than Cairnes' cataloging of mineral showings and attendant classifying of veins on the basis of potentially extractable metals. The current work is an attempt to provide a regional synthesis of veins in the district by using fluid inclusions and stable isotopes in order to indicate possible genetic relationships among them. In doing this the author hopes to provide a model which will facilitate exploration not only in the Wheaton River Valley but in other, similar areas as well.

## II. REGIONAL GEOLOGY

### A. Tectonic Assemblage

In addition to being near the border of two physiographic regions, the Wheaton River Valley also straddles the boundary between two major tectonic elements of the Cordillera, the Coast Plutonic Complex and the Intermontane Belt (Fig. 1). The Coast Plutonic Complex is considered by Monger *et al.*, (1982) to represent the juncture of two, composite allochthonous, terranes which were accreted to the ancient North American margin from mid-Jurassic to early Tertiary. The first terrane was emplaced by late Jurassic to early Cretaceous; its join with the North American craton is represented by the Omineca Crystalline Belt.

### B. Coast Plutonic Complex

The Coast Plutonic Complex began forming in Cretaceous time in response to forces associated with the accretion of the second, composite, allochthonous terrane and was essentially complete by early Tertiary (Tempelman-Kluit, 1979). The Coast Plutonic Complex is made up of predominately felsic intrusive rocks of granodioritic, dioritic and granitic compositions (Fig. 2). In the Wheaton River Valley, the Coast Plutonic Complex is represented by biotite-hornblende quartz diorite on Mt. Wheaton, Mt. Stevens, Tally-Ho Hill, Gold Hill and Mt. Anderson (Fig. 3). Hornblende-biotite-oligoclase granodiorite of the Coast Plutonic Complex makes up the bulk of Carbon Hill and Mt. Ward; and a small portion of the east face of Chieftain Hill (Wheeler, 1961).

### C. Intermontane Belt

#### Whitehorse Trough

The Intermontane Belt in Yukon is composed of two terranes, Whitehorse Trough and Yukon Crystalline Terrane (Fig. 1). Whitehorse Trough incorporates four stratigraphic units

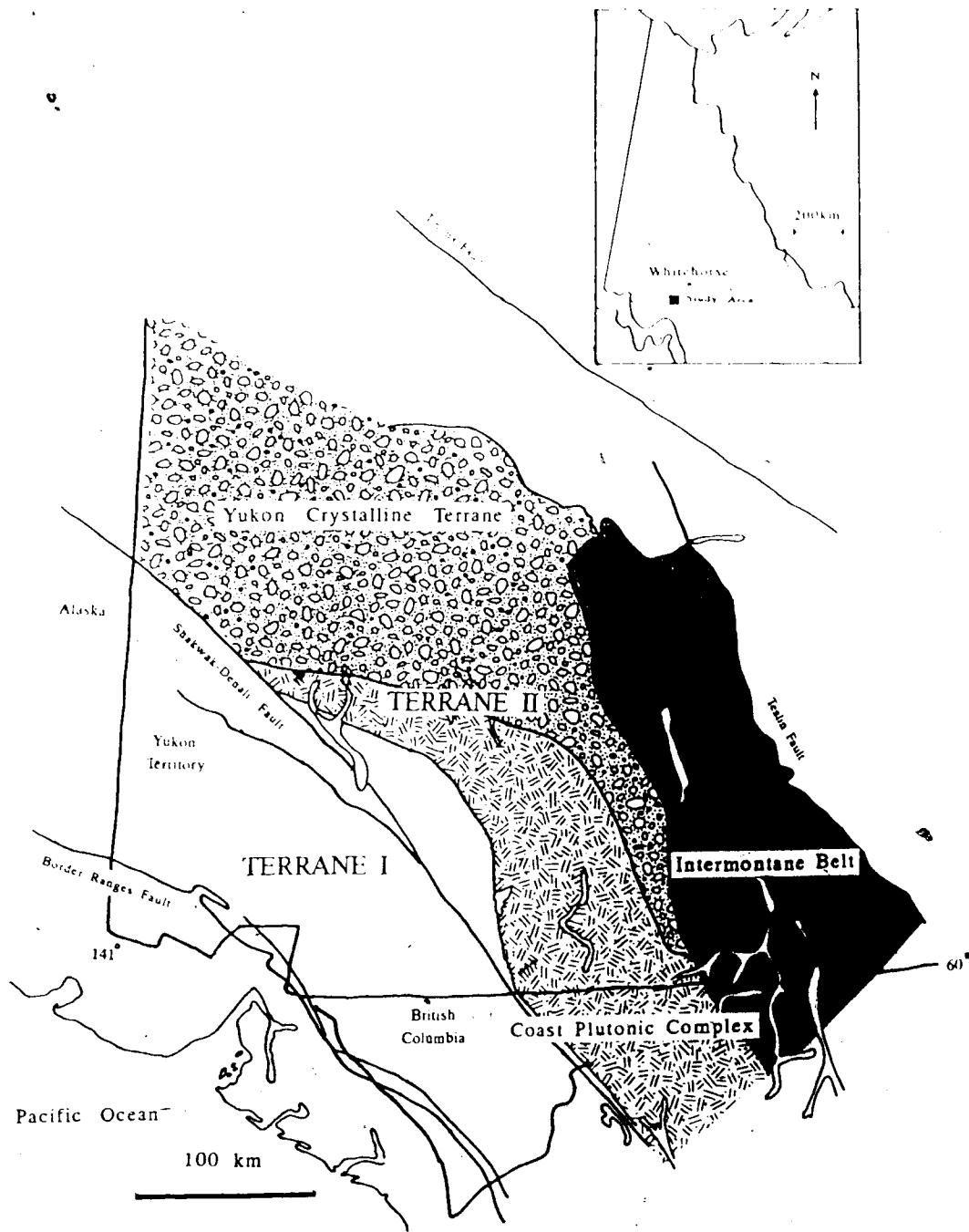


Figure.1 Tectonic assemblage map of southwestern Yukon and northwestern British Columbia, and location map of study area. Adapted after Monger et al., 1979 and Tempelman-Kluit, 1981.

in southern Yukon: Cache Creek Group, Lewes River Group, Laberge Group and Tantalus Formation. The Cache Creek Group consists of a series of basalts, cherts and carbonates of Mississippian to Triassic age, which have been subjected to high pressure metamorphism resulting locally in the production of blueschist facies rocks (Tempelman-Kluit, 1981). Melange texture is a common feature of the Cache Creek Group. These rocks are believed by Monger *et al.*, (1982), to represent a slice of oceanic crust which has been strongly metamorphosed in a subduction zone. The Lewes River Group is a thick ( $\approx 3050\text{m}$ ) sequence of interbedded sedimentary and volcanic rocks of Late Triassic age which overlies the Cache Creek Group (Wheeler, 1961). The sedimentary units of the Lewes River Group are siltstones, argillites, carbonates and conglomerates. Volcanics range from basalt to andesite, in addition to associated andesitic volcanoclastics. In addition there are rocks which can be considered transitional between the sediments and volcanics, i.e. graywackes and conglomerates with high proportions of volcanic fragments of varying size. Various greenschists and greenstone units near the boundary zone with the Coast Plutonic Complex are considered to be metamorphic equivalents of the Lewes River Group (Tempelman-Kluit, 1981). The Laberge Group is a sedimentary unit, almost as thick as the Lewes River Group, which is comprised of clastics derived from this latter group. Tempelman-Kluit (1976) considers Wheeler's (1961) criteria for separating the two on the basis of the position of a particular limestone bed to be unreliable. Since they appear to grade into one another laterally in some areas, Tempelman-Kluit believes that the two units represent a single, near-shore sedimentary sequence. Conglomerates and sandstones of early to middle Jurassic age dominate the Laberge Group. The Tantalus Formation is a 760m thick sedimentary unit of late Jurassic to early Cretaceous age, which unconformably overlies the Laberge Group. It includes arkoses, siltstones, argillites and minor coal beds, but its most easily recognisable unit is a chert pebble conglomerate whose clasts are probably derived from the Cache Creek Group (Wheeler, 1961). Taken together these four units are believed to represent the remnants of an ancient fore-arc basin, while the Coast Plutonic Complex represents the reactivated roots of that arc (Monger, et al, 1982; Tempelman-Kluit, 1979).

Of the four units mentioned above, only the Cache Creek Group is not present in the Wheaton River valley. Outcrops of Lewes River Group greenschists occur on Mt. Stevens, Tally-Ho Hill, Dickson Hill and Gold Hill, with minor exposures of carbonate and carbonate breccia on Tally-Ho and Gold Hills (Fig. 3). The Laberge Group is restricted to the cluster of peaks in the northeastern part of the area which includes Mt. Folle, Idaho Hill and Mt. Perkins. A roughly triangular body of the Tantalus Formation occurs on Mt. Folle, Mt. Bush and Idaho Hill. There are also two very limited exposures of the Tantalus Formation on Carbon Hill which is the extent of this formation in the valley.

#### Yukon Crystalline Terrane

A number of small outcrops of schistose and gneissose rocks are found on Mt. Anderson and Carbon Hill, with a body of metamorphic rocks of considerable extent occurring west of Mt. Skukum. These rocks were formerly referred to as part of the Yukon Group; however, this term was defined so loosely initially and used so indiscriminately since that further use has been discouraged (Tempelman-Kluit, 1976). The rocks are now considered to be part of the Yukon Crystalline Terrane, a tectonic element which includes a number of metamorphic units that had various names in the past, e.g. Pelly Gneiss, Klondike Schist and Nasina Quartzite. The terrane is comprised of at least four units, biotite schist, marble, graphitic quartzite and amphibolite, all of unknown age. They are generally believed to be at least Paleozoic in age, with the possibility that the sediments were originally deposited in Precambrian time. Radiometric dating of these rocks indicates at least six thermal events beginning in Mississippian time and continuing through early Tertiary (Tempelman-Kluit and Wanless, 1975; Wilson *et al.*, 1985). The relationship of the Yukon Crystalline Terrane rocks to the Whitehorse Trough rocks is unclear, though the volcanic roots of the Lewes River Group are known to intrude the Yukon Crystalline Terrane metamorphics. There is speculation that the Whitehorse Trough sediments may have been deposited on the Yukon Crystalline Terrane rocks, but this is by no means certain, due to the fact that their field relations have been obscured by faulting and erosion (Tempelman-Kluit, 1981).





## D. Volcanic Units

### Skukum Group

Other than unconsolidated Quaternary material on the valley floors, only two other geologic units are found in the Wheaton River valley. Both units are composed primarily of volcanics, volcanoclastics and volcanic derived sediments. The first is the Skukum Group which makes up the Skukum Volcanic Complex, a Tertiary volcanic center, in the northwestern part of the district that contains rocks of andesitic to rhyolitic composition (Pride, 1986). The complex is composed of various tuffs, agglomerates and flows, as well as minor water-lain beds, which have all been heavily faulted. The Skukum Volcanics unconformably overlie rocks of the Coast Plutonic Complex and Yukon Crystalline Terrane. In addition to Mt. Skukum, the Skukum Group Volcanics are found on Vesuvius Hill, Gold Hill, Chieftain Hill and Mt. Reid. A number of small discordant rhyolite plutons present on Mt. Skukum, as well as Carbon Hill, Mt. Anderson, Mt. Folle and Gold Hill have been correlated with the Skukum Group Volcanics (Smith, 1983). The rocks of the Bennett Lake Cauldron Complex, approximately 25km south of Mt. Skukum, are similar in age and are also considered to be part of the Skukum Group, which is in turn part of the Sloko Volcanic Province of the northern Cordillera (Pride, 1986).

### Mesozoic Volcanics

A second volcanic unit, formed in large part by mafic flows and breccias, is found in outcrop on Mt. Stevens, Mt. Wheaton, Mt. Bush and Mt. Perkins. It has no formal name, being most often referred to as simply "the Mesozoic volcanics". Its relationship to other units is unclear, although some writers feel that it may be part of the Lewes River Group, others consider it to be part of the Hutshi or Mt. Nansen Groups of volcanics (Cockfield and Bell, 1944; Wheeler, 1961; Tempelman-Kluit, 1981). Grond *et al.*, (1984) have assigned a late Cretaceous age to the Hutshi and Mt. Nansen Groups.

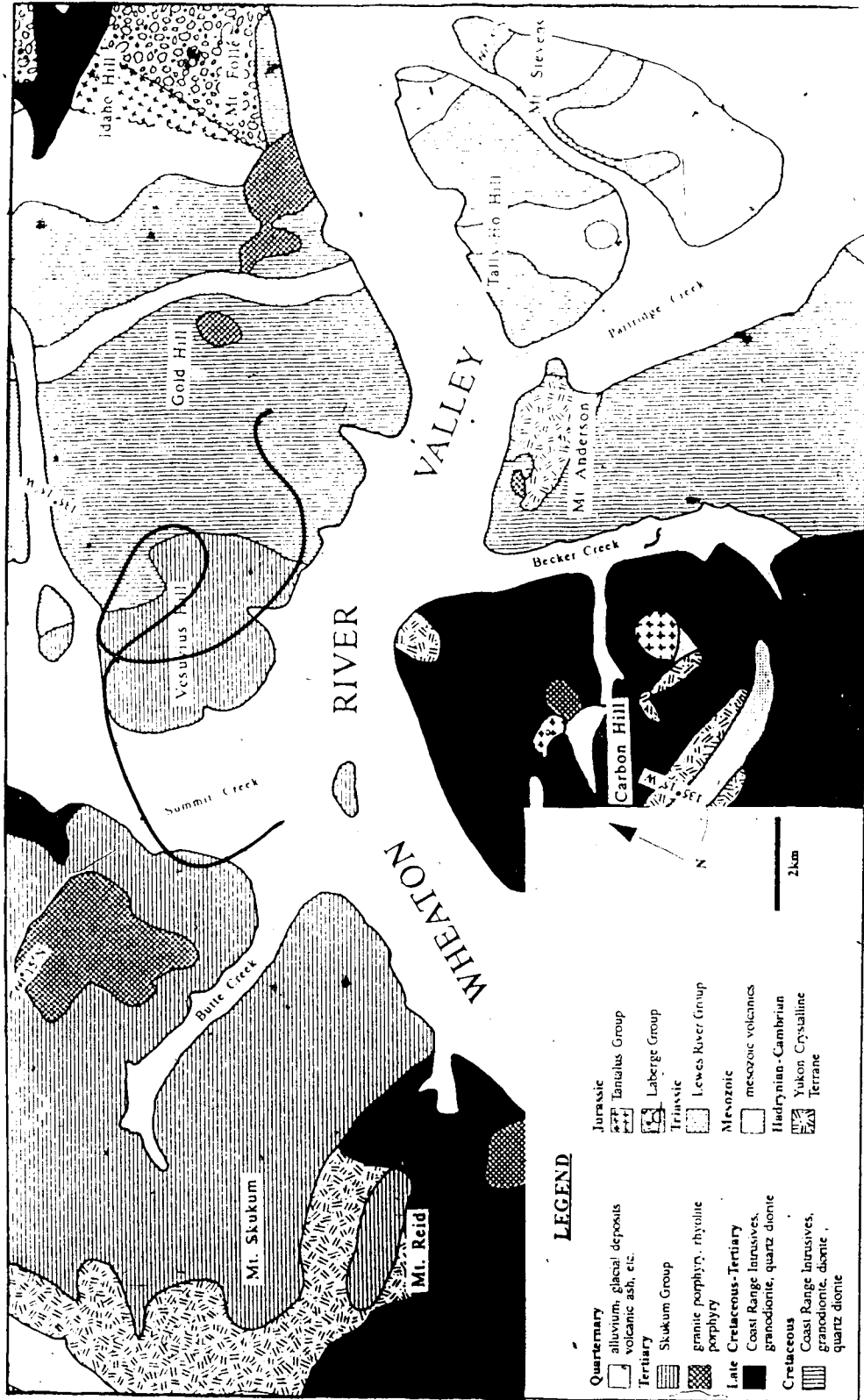


Figure.3 Geology of the Wheaton River Valley with locations indicated of principal peaks. Modified after Wheeler, 1961.

### E. Regional Structural Trends

As can be seen from the accompanying geologic map the major tectonic elements of the southern Yukon all trend northwest-southeast. This trend is reflected in the cleavage traces of the metamorphic rocks of the Lewes River Group and Yukon Crystalline Terrane as well as the fold axes of these rocks. This trend is one piece of evidence which led Monger *et al.*, (1979) to conclude that allochthonous terranes have accreted to the North American craton from the southwest over time. Faults of limited extent are found in a number of places in the valley but as of this writing no major throughgoing fracture has been discovered in the immediate vicinity. These minor faults may serve to separate one geologic unit from another or they may be wholly within a single unit. They often serve as the hosts for the mineralized veins, which are the subject of this study.

### III. MINERAL OCCURRENCES

#### A. Introduction

Mineral showings occur on nearly all of the major peaks which form the valley walls, including Klabo Hill, Mt. Folle, Mt. Wheaton, Lally Ho Hill, Mt. Stevens, Dickson Hill, Gold Hill, Mt. Anderson, Carbon Hill, Mt. Reid and Chieftain Hill (Fig. 4). The showings consist of sulfide-bearing quartz veins which, in the past (Carnes, 1912), were categorized simply on the basis of the metals of primary economic interest contained in each. The vein types which this categorization gave rise to are gold-silver, silver-lead and antimony-silver. The veins are hosted by granitic rocks of the Coast Plutonic Complex, by Lewes River Group metamorphics, by Eaberg Group sediments and by Mesozoic volcanics of undetermined affinity. Quartz is by far the dominant gangue mineral in all of these veins with calcite and, very rarely, barite being only locally important. Metallic minerals include pyrite, galena, stibnite, arsenopyrite, sphalerite, and pyrrhotite among others. Tellurides and native gold have been reported from various showings, however, none were seen during the course of this study. The various mineral showings throughout the district have been given many different names over the years as new companies or individuals became interested in them. In the descriptions of specific showings, I have attempted to use those names which were in broadest use among those working the valley in 1985.

#### B. Stibnite-bearing Veins

##### Yukon Antimony

The three major properties on Carbon Hill are Yukon Antimony (Becker-Cochran) on the east side of the hill at the head of a deeply incised tributary of Becker Creek, Porter claims on the west face above Antimony Creek and Goddell's claim on the north face from an elevation of 1250m to 1480m. The Yukon Antimony consists of stibnite bearing vein material in a shear zone. Abundant evidence of surface workings is present over a large area; however,

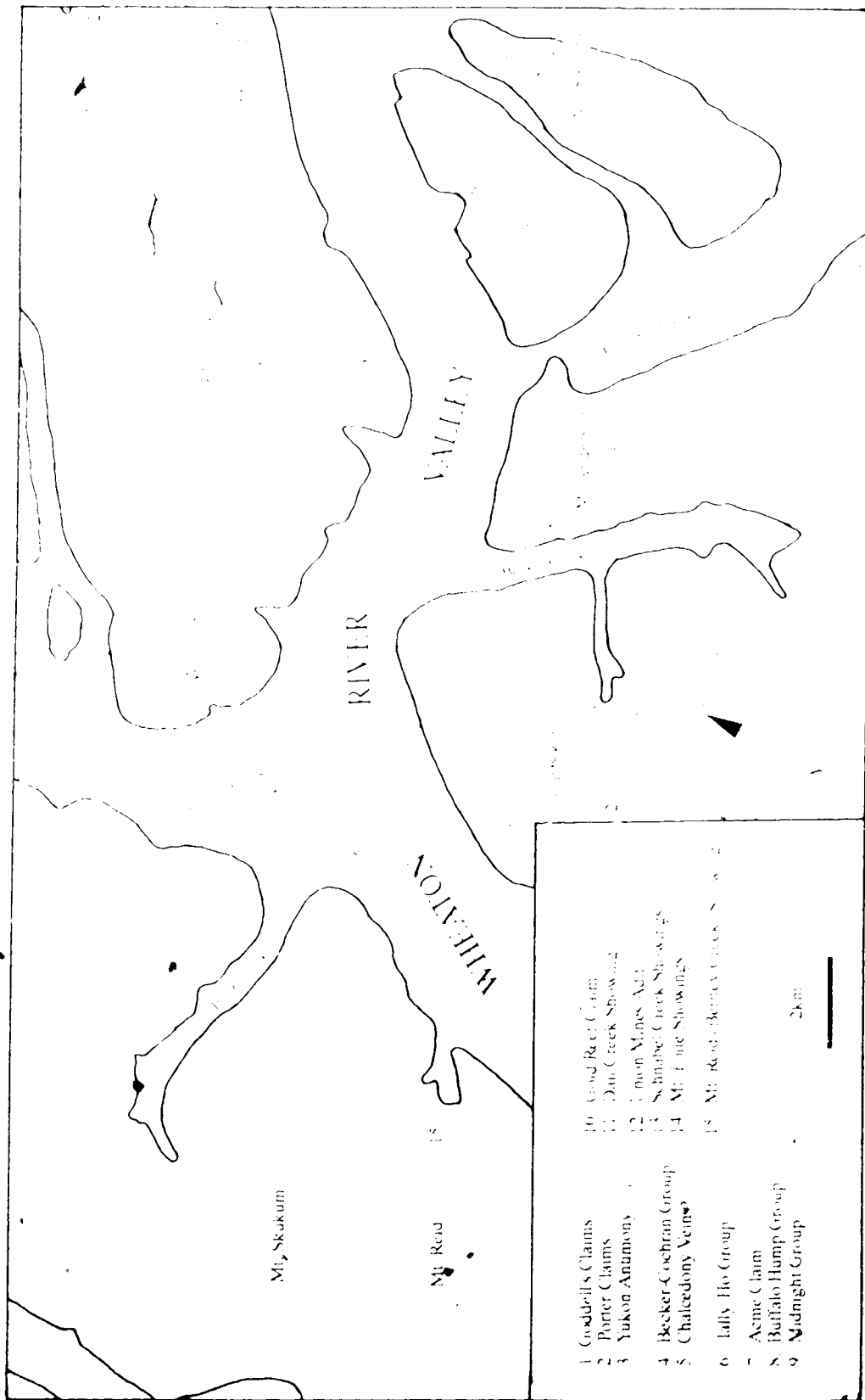


Figure 4 Map showing locations of the principal mineral occurrences in the Wheaton River Valley.

all old trenches have slumped to the point that no information could be gained from them. On the other hand, one major adit and one minor one are still open. The shear zone is not evident on surface, but previous workers (Havlands, 1966) report that on stripping it was found to extend 305m with an average width of about 2.1m. The strike of the shear is 130° with a steep southwesterly dip generally exceeding 65°. The zone appears to be related to a large rhyolite dike which serves as the footwall throughout its length. The hanging wall lithology varies considerably with rhyolite, Tantalus conglomerate and andesite being reported. The rhyolite and andesite are part of the unnamed Mesozoic volcanic unit. The dike is typically brecciated and altered adjacent to the shear. Alteration consists of carbonatization of feldspars, minor sericitization and extensive silicification throughout; even rhyolite that appears relatively fresh is heavily silicified. The material within the shear is primarily gouge which is light gray in color and very sticky to the touch. Mineralization is discontinuous consisting of massive pods and stringers of material of varying proportions of sulfides and gangue. Presumably the volcanics and sediments, which host the shear, exist as a pendant to the Ruby Range granodiorite, which comprises the bulk of Carbon Hill; whether the shear penetrates downward into the granodiorite is unknown.

### Porter Claims

The Porter claims are marked by an adit at about the 1600m level on the west face of Carbon Hill. Since all surface trenching had slumped long ago this adit functions as the only access to mineralization. The showing consists of a stibnite-bearing quartz vein hosted in Ruby Range granodiorite. The tunnel cuts a series of minor subparallel (strike  $\approx 113^\circ$ ) shears of variable dip. These shears, the widest of which does not exceed 0.75m, are characterized by light gray clayey gouge. Three crosscuts, two only minor, have been made at intervals along the main tunnel, each of which appears to follow a shear. A small, barren quartz vein is present in the first crosscut. The third and by far largest crosscut contains the only showing of stibnite in the workings. The showing,  $\approx 3$ m long, is an 8-10cm wide vein of massive stibnite and quartz that appears to be terminated by the shear. The tunnel is cut by two

andesite dikes one near the portal, the other at the far end. The strike of the first is 063°, dipping vertically, and the second 104°, dipping 22° SW.

### **Goddell's Claims**

Goddell's Claims on the north face of Carbon Hill were the most poorly exposed of this group of stibnite-bearing veins. Only one small vein,  $\approx 12$ cm wide, was exposed near an access road cut to several old drill pads. This vein was hosted in heavily altered granodiorite. Although extensive talus cover prevented further determination of the geology immediately adjacent to the vein, the vein was seen to be near the lower contact of the Mesozoic volcanics with the Ruby Range granodiorite. In addition, an outcrop assumed to be an exposure of the vein was discovered near the summit of the north face of the hill. The exposure apparently has not been noted in any of the old literature. This outcrop is near the beginning of the access road mentioned earlier and may have been uncovered during its construction. The host in this case is an andesite prophyry unit of the Mesozoic volcanics.

### **C. Galena-bearing Veins**

#### **Mt. Anderson**

Only two significant vein occurrences are present on Mt. Anderson. The first is an extensive, galena-bearing, massive, quartz vein which was studied thoroughly by D.R. Bull (1986). The vein is hosted in Ruby Range granodiorite and is associated for most of its length with a basalt dike that runs parallel to it. Extensive gouge exists between the vein and its host rock and also between the dike and the host. The strike of the vein is  $\approx 105^\circ$  with a dip of  $85^\circ$  S. The second vein occurrence is found in a trench on the second knoll south of the north face of Mt. Anderson. Many old trenches exist on the summit, but most have slumped to an extent that they are useless without major re-excavation; however, in this case the walls possess sufficient integrity that features are still clearly discernible. The showing consists of one main vein (strike  $103^\circ$ , dip  $48^\circ$  S) approximately 46cm thick, which is composed of fine

grained quartz with a number of small stringers that run along the trench wall. The stringers can be traced for 4m to a large mafic pod where they trace its outline (even penetrating its outer surface) and thence 2m to a chalcidony and breccia vein. The host rock in all cases is heavily weathered granodiorite that actually crumbles in the fingers.

#### **Mt. Stevens**

Three occurrences of vein outcrops were located on Mt. Stevens in 1985. These occurrences are believed to correspond to three old claim blocks, i.e. Buffalo Hump Group, Acme Claim and Midnight Group. The Buffalo Hump showing was found in fresh bulldozer workings near the summit. The showing consists of a pod of massive galena in a quartz vein having a total thickness of 2.5m and striking at 146°. The vein, exposed for only a short distance, is hosted in highly altered granodiorite. The presence or absence of gouge could not be determined due to extreme weathering. The Acme showing ≈200m SE of the Buffalo Hump Group consists of a large (10m x 30m), sparsely mineralized quartz lens hosted by Lewes River Group schists. The lens is elongated parallel to the foliation in the schist which in this case strikes at 133°. The Midnight Group showing is located just north of the small valley separating Mt. Stevens from Dickson Hill on the east face of the former. This showing is unique in the valley in that it is not made up of one or more relatively large quartz veins, rather it is composed primarily of a granite porphyry dike which has been brecciated by cross-faulting. The breccia fragments are heavily altered and cemented by a myriad of sporadically mineralized quartz veinlets. The host for the dike is, again, Lewes River Group greenschist.

#### **Tally-Ho Hill**

Only one showing is present on Tally-Ho Hill, the Tally-Ho Gulch property on the north face of the hill at ≈1400m. The showing is reported to contain a galena-bearing vein up to 85cm wide occurring in a brecciated fault zone in granodiorite. Caving of the old workings prevented any direct observation of the the vein. However, much quartz float present near the



portal was presumed to be waste from the workings. In addition, a small quartz-carbonate vein hosted in greenschist was located about 17m NW of the portal.

### **Gold Hill**

The Gold Reef claim and Dail Creek showing are located on Gold Hill, the former in a draw on the northeast side of the hill at 1680m and the latter at the head of Dail Creek at 1460m. At the Gold Reef Claim, all old workings again were caved, but quartz waste was abundant below the old adit. The vein is hosted in greenschist and was reportedly traced for over 300m by previous workers. The vein, said to average about 1.5m in width, parallels the foliation in the schist, striking 125°. It was also reported that the vein would cut across the foliation intermittently then resume its parallel relationship. The Dail Creek showing has never been worked extensively. It is comprised of a single exposure of highly weathered quartz vein material and equally weathered granodiorite host rock. The vein, striking 109° and dipping 78° S, varies in width from 47cm to 22cm over an exposed distance of ≈2m. A number of small quartz stringers are found adjacent to the vein.

### **Mt. Reid**

Two veins have been reported on Mt. Reid, but as in previous instances slumping and caving of old workings prevented detailed examination of the veins. Fortunately, one outcrop of galena bearing quartz was located above old portal timbers. This outcrop was intensely weathered, bearing a great deal of iron oxide crust and stain. Earlier reports state that gouge and vein matter in this vein totalled 4.5m in width, this seems likely since the gully in which the outcrop is located appears to be filled with weathered gouge from one granodiorite wall to the other. Andesite is found on the west side of the gully near the summit and the shear reportedly cuts andesite at depth. The andesite is thought to be part of the Skukum Complex.

#### D. Arsenopyrite-bearing Veins

Veins whose dominant sulfide mineral is arsenopyrite are found primarily on Idaho Hill and to a much lesser extent on Mt. Folle. The veins are hosted in the Laberge Group and are often seen to replace the wallrock. Two principal showings are present, both on the old Export Union Mines group of claims. The first consists of a number of veins of varying widths exposed in the old Union Mines adit, at 1070m on the southeast face of Idaho Hill. The veins strike northwesterly and dip steeply west. They generally follow fractures in the graywacke host and carry little or no quartz. The second showing is in Schnabel Creek Canyon at the base of Idaho Hill ≈1km upstream from a pair of cabins. In this location a great deal of banded vein material was found lying beside a bulldozer road. This material was supposedly taken from a 50cm vein uncovered by the bulldozer during construction of the road. The vein was subsequently recovered, meaning that no actual outcrop was seen. A number of small veins were located in several places on Idaho Hill and Mt. Folle, other than variable proportions of sulfides, they are unremarkable.

## IV. MINERALOGY AND PETROLOGY

### A. Introduction

The sulfide-bearing quartz veins of the Wheaton valley were divided by Cairnes (1912) into three types according to the metals of primary interest in each. The three types were antimony-silver, gold-silver and silver-lead veins. In light of the fact that the sulfide mineralogy of each of these types is dominated by a single mineral, it is felt that classifying the veins according to the dominant mineral is more appropriate to the study at hand. Stibnite is the dominant mineral of the antimony-silver veins. Silver values in these veins were reported to be highest where galena and tetrahedrite were most abundant and stibnite was relatively scarce (Cairnes, 1912; Cockfield and Bell, 1944). These veins are found on Carbon Hill with additional showings reported on Chieftain Hill. Unfortunately, the author could not locate any vein outcrops on Chieftain Hill. The gold-silver veins are dominated by galena with pyrite nearly as abundant in a few instances. Gold and silver values were said to be highest when galena was present; the actual amount of galena apparently being irrelevant. Gold was present as the native metal or associated with tellurides. Neither occurrence of gold was observed by the author. Galena-bearing veins are present in a number of localities. The sulfide mineralogy of the silver-lead veins is dominated by arsenopyrite. Silver values, again, are highest where galena is present. These veins are found in the Idaho Hill-Mt. Folle area. Exceptions to this classification do occur in the valley; they will be discussed where appropriate in the following descriptions of the mineralogy and petrology of the various showings.

### B. Stibnite-bearing Veins

#### Host-rock Petrology

The stibnite-bearing veins of Carbon Hill are hosted in Ruby Range granodiorite (Porter adit, Goddell's Claims) and Mesozoic volcanics (Yukon Antimony). In both instances

where underground access was possible, mineralization was seen to be associated with shearing in the host rock. The shearing is evidenced by the presence of variable amounts of sticky gray gouge and the development of slickensides. Mineralization may occur anywhere in the shear zone.

Granodiorite samples whether taken adjacent to a vein or some distance from one are extensively altered. While the original texture and minerals are easily recognizable, alteration is pervasive with all primary minerals being affected to one degree or another. Most of the plagioclase has been converted to a fine-grained mixture of calcite and sericite with only a few unaltered areas remaining. Measurements done on the few relatively fresh areas indicate a plagioclase composition of  $\approx An_{30}$ . Perthitic orthoclase has not been as heavily altered as plagioclase but it does have a very cloudy appearance due to sericitic alteration. Hornblende and biotite, the typical mafic minerals of a granodiorite, were not observed; however, the combination of muscovite and iron oxides, which is presumed to be their alteration assemblage, is present throughout. Secondary quartz, which is ubiquitous, forms a graphic intergrowth with the feldspars. At times this intergrowth appears myrmekitic. The feldspars (usually plagioclase, but occasionally orthoclase also) are embayed or enclosed by optically continuous quartz. The graphic texture of quartz and embayment of feldspars suggest that quartz generally replaces feldspars throughout the granodiorite host. In addition to carbonate in altered plagioclase, numerous small carbonate veinlets are found throughout the unit. The pervasiveness and uniformity of alteration in the granodiorite, regardless of distance from mineralization, implies that the alteration is not closely related to the mineralization or, at least, it had no controlling effect on mineralization.

Three rock types serve to host the mineralized shear on the Yukon Antimony property. The first and most important is a rhyolite dike which is associated with the Mesozoic volcanics. This dike constitutes the footwall of the shear over its entire explored length as well as a major portion of the hanging wall (Hylands, 1966). The dike is heavily fractured near the vein and shows copious iron oxide staining. The rhyolite is porphyritic, with phenocrysts consisting of albite that have been altered to sericite and carbonate. Small

clusters of sericite, carbonate and iron oxides, which may be alteration products of the original mafic minerals, are present throughout. The matrix is extremely fine-grained with disseminated quartz and sericite inclusions. The second type of host rock for the Yukon Antimony vein is Skukum rhyolite, which is present in the form of two dikes that intrude the shear zone. In hand specimen this rhyolite looks rather similar to the unit previously described, being heavily iron-stained and slightly porphyritic, but in thin section the differences between the two rock units are clear. The Skukum rhyolite has been extensively silicified to the point that the rock consists of over 75% secondary silica nearest the shear zone. This silica has abundant inclusions of secondary plagioclase. Sericitic alteration of both primary and secondary plagioclase is much less pronounced in this rock and secondary carbonate is lacking. Mafic minerals again are absent. Iron oxides are concentrated with sericite along fractures and, also occur as rare pseudomorphs after pyrite cubes. The groundmass is a felted mass of orthoclase, plagioclase and quartz. The third rock type hosting the shear zone is the Tantalus conglomerate. As the contact of the conglomerate with the shear zone is very limited and likely has no bearing on mineralization, no detailed description will be presented here.

## **Vein Mineralogy and Petrology**

The mineralogy and petrology of the stibnite veins are relatively simple. In the Yukon Antimony samples the only sulfides identified were stibnite, sphalerite and very minor pyrite. The gangue consists of quartz and barite. The quartz exhibits coarse anhedral to euhedral morphologies that were corroded sometime after initial formation. Stibnite, often including small euhedral barite crystals, filled in the interstices of this corroded quartz. It would seem likely that the stibnite is replacing the quartz. The relative abundances of stibnite and quartz vary widely in the vein with the common occurrence of large masses of stibnite containing only scattered quartz grains. Sphalerite is light reddish brown in color and is found only near the contact of the vein, with the wall rocks. The sphalerite tends to be fractured and, when stibnite is present, is apparently replaced by the latter mineral to a limited extent. Pyrite is

normally present as widely scattered cubes in quartz and/or stibnite. In one sample pyrite forms a few small stringers in stibnite. Barite, as well as being present as isolated euhedra in stibnite, forms the dominant gangue mineral in a few instances. In these instances it is present in the form of large (>3cm) blades with interstitial quartz. Late movement in the shear zone has caused minor brecciation of both gangue and sulfides in some places.

The vein material occurring in the granodiorite is somewhat more complicated mineralogically and texturally. Only one additional sulfide mineral associated with stibnite was identified, namely jamesonite. Also, galena was identified in a specimen from a minor veinlet in the Porter adit, but no other sulfides were present with it. On the other hand, barite was rare being found in only one location on Goddell's Claims. The complexity in this material arises from the intergrowth of quartz and stibnite. Two generations of quartz are clearly evident in these samples. The first generation is composed of relatively coarse quartz and exhibiting a high degree of euhedral development. The second generation occurs both as fine-grained overgrowths on the first generation and as distinct anhedral grains, in both instances having an obvious radial growth pattern (Plate. 1). Aggregates of stibnite needles can be seen to form concentric bands in some quartz grains probably outlining growth zones in the grain (Plate. 2). In other instances, stibnite is clearly replacing the second generation quartz, where the former occurs interstitial to the latter. The evidence of replacement is in the concave boundaries of the quartz and in the projection of individual stibnite needles into the quartz (Plate. 3). Sphalerite is again present only near the wallrock contact and is replaced by stibnite to a greater degree than in the Yukon Antimony samples. Jamesonite occurs as isolated grains in stibnite.

### **Paragenesis**

The paragenetic sequence of the stibnite-bearing veins (Fig. 5) was initiated by the deposition of coarse-grained anhedral to euhedral quartz. Sphalerite was deposited early in this stage since it occurs only in the quartz near the wallrock. A second generation of finer-grained quartz was deposited next in the form of overgrowths on the original quartz, as

Stibnite-bearing veins

Quartz(I)

Sphalerite

Pyrite

Quartz(II)

Stibnite

Jamesonite

Barite

Figure.5 Idealized paragenetic sequence of the stibnite-bearing veins.

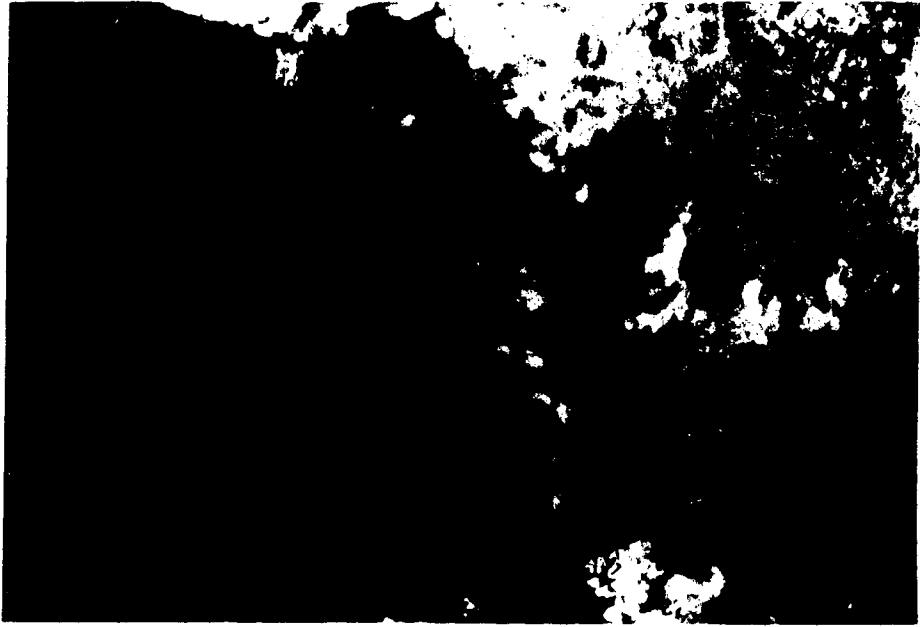


Plate.1 Radial growth pattern of second generation quartz on first generation quartz core.  
Field of view is 1.5mm.





Plate.2 Stibnite needles outlining growth zones in quartz from the Porter adit. Field of view is 1.5mm.

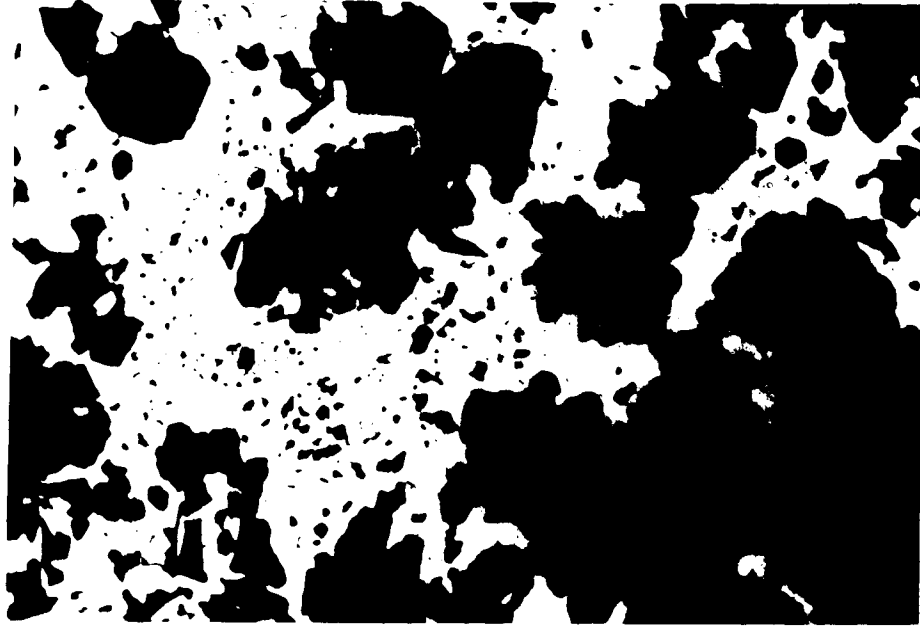


Plate 3 Fine grained stibnite embaying quartz grains from Goddell's Claims. Field of view is 1.5mm

well as, interstitial grains. Stibnite deposition appears to have commenced sometime after the onset of the second generation quartz and continued to be deposited until mineralization ceased. The stibnite clearly replaces first and second generation quartz in some instances, while, at other times, it simply fills the interstices in the second generation. The concentric banding of stibnite in quartz further confirms contemporaneous deposition. It may indicate an alternating sequence of deposition of quartz and stibnite, but this could not be confirmed on a larger scale. Jamesonite is contemporaneous with the stibnite as it occurs only as isolated grains in the latter mineral. Barite was also deposited at the same time as the stibnite as evidenced by the presence of barite euhedra in coarse stibnite which is interstitial to quartz. It is not clear what the relationship of the galena identified in the veinlet in the Potter adit has to the stibnite mineralization but it replaces coarse, anhedral quartz in this veinlet.

### C. Galena-bearing Veins

#### Host-rock Petrology

Galena-bearing veins are hosted in Ruby Range granitic rocks and Lewis River Group metamorphic rocks. Alteration in the granitic rocks is similar to that observed associated with the stibnite-bearing veins (Plates 4 and 5). In this case it varies to a limited extent, with distance from vein mineralization. Alteration takes the form of sericitization of feldspars (always more intense for plagioclase) and, chloritization and carbonatization of amphibole and biotite. The sequence of samples from the Mt. Anderson adit studied by Bull (1986) indicates a marked intensification of alteration immediately adjacent to the vein. This sequence of samples is valuable because the excellent access provided by the adit on this property permitted the systematic sampling of the host rock at ever increasing intervals from the vein. Unfortunately, such a clearly defined sequence of samples could not be duplicated with any certainty on any other showing but the alteration trend indicated on Mt. Anderson seems to hold true, at least broadly, for the other localities where granodiorite or quartz diorite is the host rock; i.e. Buffalo Hump Group, Tally-Ho Gulch, Dail Creek and Mt. Reid.

As it was not possible to ascertain whether or not a particular schist sample was actually representative of the true immediate host rock for any single vein on Mt. Stevens or Gold Hill, a brief description of the three prevalent rock types will be given. The first is a schist found near the Acme showing on Mt. Stevens. This rock is composed for the most part of fine-grained quartz; schistosity is defined by layers of sericite. Small carbonate veinlets parallel the sericite at intervals. A few, large, rounded quartz grains are present, presumably relicts from the sedimentary precursor. Iron oxides are abundant throughout. The second rock is essentially an aggregate of alteration minerals produced by the alteration of a mafic porphyry. No relict grains remain and phenocryst outlines are too indistinct to permit definitive conclusions as to their origins. The altered phenocrysts are now masses of Mg-rich chlorite or sericite; while the groundmass is a mixture of Fe-rich chlorite, sericite, carbonate and iron oxides. A number of roughly parallel carbonate veinlets, sometimes containing considerable amounts of epidote, cut the unit. The third rock type is a fine-grained, chlorite-sericite schist also cut by carbonate veinlets. A few, small, relict grains of quartz and plagioclase are still recognizable while other grains are completely sericitized. Iron oxides are disseminated throughout.

### **Vein Mineralogy and Petrology**

#### **Mt. Anderson**

The mineralogy of the galena-bearing quartz veins is more variable than the stibnite-bearing veins. The most complete and best documented suite of samples was obtained by D. Bull on Mt. Anderson. These samples appear to indicate a single episode of deposition in which quartz and adularia were deposited more or less continuously, while sulfides were deposited intermittently. The gangue minerals are coarse and intergrown, showing little or no replacement textures. Secondary veinlets, normally filled with fine-grained quartz or occasionally carbonate, cut the coarse-grained gangue in some places. Sulfide minerals occur as discontinuous pods and lenses almost anywhere in the body of the vein, though generally they are found to be more often toward the center,

These pods are made up of variable amounts of galena, sphalerite, pyrite and chalcopyrite. Tetrahedrite occurs sporadically and native gold was reported in two samples from a trench which exposed the vein  $\approx$ 130m above the lower adit. The relative proportion of galena decreases in these samples while that of pyrite increases, as compared to material from the adit. Galena was observed to replace pyrite, while sphalerite replaces both of these. Pyrite tends to be brecciated, while chalcopyrite and tetrahedrite occurs as blebs in sphalerite and galena respectively. In addition, chalcopyrite is found as anhedral grains and stringers filling in around galena and quartz.

The fine grained quartz and chalcedony veins found by the author on a knoll south of the main showing carry no sulfides, but fluorite and chalcedony pseudomorphs after fluorite are present. The fluorite is very light green in color and occurs at the margin of the vein. Where granodiorite breccia is abundant in the veins, quartz has grown radially from the fragments developing a very elongate prismatic habit. In some instances milky, banded chalcedony has formed at the terminal ends of the radiating quartz clusters. The relationship of these veins to the main showing is not clear, but the presence of chalcedony and fluorite suggest that these veins represent the upper portions of a hydrothermal system (Fournier, 1985).

#### Mt. Stevens

Vein materials obtained on Mt. Stevens differs slightly from that found on Mt. Anderson in both gangue and sulfide mineralogy. The gangue in these materials is composed entirely of massive, coarse-grained quartz regardless of the host rock. In places the vein material shows signs of having been brecciated and recrystallized with the introduction of minor sericite. The only primary sulfides identified were galena, pyrite and chalcopyrite. The massive galena pod found on the Buffalo Hump Group claims, which apparently fills a large vug in the vein, contains only minor pyrite and chalcopyrite in the form of blebs and rare stringers in the galena. The secondary copper minerals covellite and brochantite are present in amounts that seem to belie the apparent paucity of chalcopyrite. The galena, which often encloses coarse hexagonal quartz is heavily

encrusted by cerussite and iron oxide alteration (Plate. 6). Only widely scattered galena grains in massive quartz gangue are found at the margins of the vein on the Acme showing; these are not accompanied by any other sulfides.

#### Gold Hill

Vein material from Gold Hill and Dail Creek is very similar to that from Mt Stevens. The gangue consists entirely of massive, coarse-grained quartz. Sulfide mineralization is composed of highly disseminated pyrite and galena. Pyrite is the only sulfide found in the Gold Hill samples. It occurs in coarse-grained clusters of as small cubes along fractures in addition to being widely disseminated in the quartz gangue.

#### Tally-Ho Hill

Material from Tally-Ho Hill collected by the author is not mineralized and consists of massive, coarse-grained quartz. As was mentioned before, a small, coarse-grained carbonate vein was located on Tally-Ho Hill as was a small amount of material comprised of highly altered granitic breccia in a chalcedony matrix.

#### Mt. Reid

The Mt. Reid showing has traditionally been included by Cairnes (1912) and others (Cockfield and Bell, 1944; Wheeler, 1961) with the veins in the valley which are of interest for their gold content that correspond to the galena-bearing veins of this study. The vein is unique, however, in that it is the only gold showing in the valley that has arsenopyrite as its dominant sulfide. Pyrite, galena, tetrahedrite and sphalerite are also present. Relative proportions of the sulfides vary among the samples but only pyrite or galena rival arsenopyrite in abundance in any one sample. Arsenopyrite and pyrite are extensively brecciated, with fractures most often filled by quartz. Tetrahedrite and galena also fill the fractures and appear to have slightly replaced both arsenopyrite and pyrite. Galena also seems to replace tetrahedrite. Chalcopyrite is only present as blebs in the tetrahedrite. Sphalerite, containing pyrite blebs, is rare and occurs as a fracture filling in arsenopyrite and pyrite. The gangue consists solely of quartz, which is vuggy and



Plate.6 Heavily corroded galena (white) from Mt. Stevens showing. Field of view is 1.5mm.

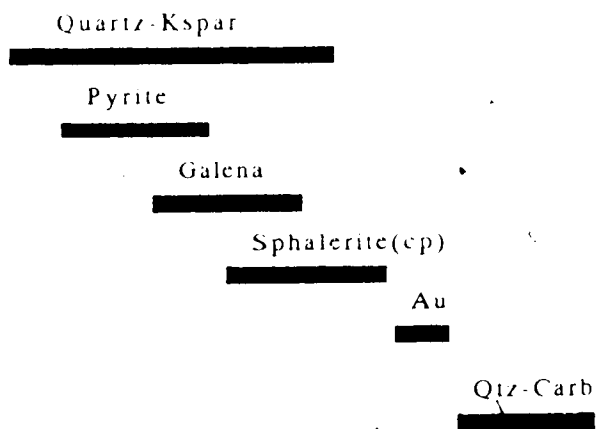
finer-grained than that of the other galena-bearing veins. Sulfides are normally present as a series of subparallel stringers in the quartz, with disseminated grains and small masses also noted.

### Paragenesis

The scarcity of well mineralized samples from the galena-bearing veins and the variability of the mineralogy in the samples that are available makes the compilation of a representative paragenetic sequence for these veins difficult (Fig. 6). The depositional sequence in the galena-bearing vein on Mt. Anderson is dominated by the deposition of the quartz-adularia gangue which continued throughout the period of primary mineralization. Sulfide pods were deposited sporadically during the gangue deposition. The first major sulfide to be deposited was pyrite followed by galena, then sphalerite. Tetrahedrite is contemporaneous with galena as it occurs as blebs in the latter mineral. Chalcopyrite and sphalerite are contemporaneous for similar reasons. One of the two reported occurrences of gold in this material is in a fracture in sphalerite indicating that gold was deposited relatively late. The veinlets of fine-grained quartz and carbonate are the final step in the depositional sequence since they cut both gangue and sulfides. The vein material from Mt. Reid also indicates continuous deposition of the quartz gangue throughout the period of mineralization. Sulfide deposition began with arsenopyrite and pyrite. These two minerals, though they are not closely intergrown, are probably coeval because they are similarly brecciated and show no obvious replacement textures with respect to one another. Tetrahedrite was deposited next followed by galena. Sphalerite is definitely later than arsenopyrite and pyrite, but its relationship to the other sulfides is not clear as it was not found in contact with them. Little can be inferred from the material from the other galena-bearing veins because sulfide mineralization is sparse. In each case it appears that deposition of the gangue occurred as a single continuous event with generally disseminated sulfides deposited intermittently. The galena pod from the Buffalo Hump Group is the only important sulfide mineralization from these showings. But even in this case only one period of deposition is indicated since pyrite



Galena-bearing veins (Mt. Anderson)



(Mt. Reid).

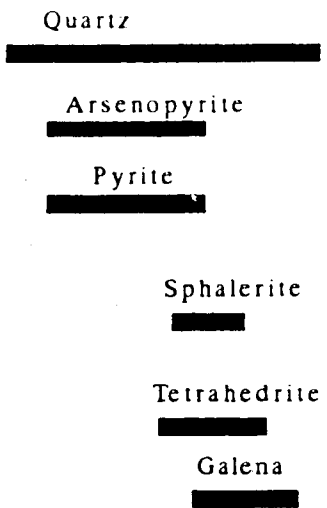


Figure.6 Idealized paragenetic sequences of two galena-bearing veins.

and chalcopyrite only occur as blebs and rare stringers in the galena.

#### D. Arsenopyrite-bearing Veins

##### Host rock Petrology

The host rocks of the arsenopyrite-bearing veins in the Idaho Hill-Mt. Folle area are various units of the Laberge Group sedimentary rocks. The hosts, which were probably arenites and greywackes originally, have undergone such intense silicification that their precursor rocks may only be hypothesized. Primary, rounded quartz clasts are surrounded by secondary silica and minor sericite. Combined primary and secondary silica often make up more than 80% of the rock. Rounded clusters of sericite and carbonate, or chlorite and carbonate at times constitute a significant portion of the rock, but more often they are only minor constituents. In addition to silicification, the host rocks are normally abundantly mineralized by disseminated sphalerite and pyrrhotite.

##### Vein Mineralogy and Petrology

Even though the veins in the Idaho Hill-Mt. Folle area are referred to in this study as arsenopyrite-bearing, the mineralogy of the veins is in fact variable to a certain extent. All of the principal showings described in the older literature contain arsenopyrite as a major constituent; if not the predominant one. During the summer of 1985, the author sampled several minor veins in which arsenopyrite was rare or even absent entirely. Some of these veins were pointed out by D. Baird, the current claimholder in this area. Because of their close spatial association with the latter veins, the textural similarities of the sulfides that are common to both, and the apparent relatively limited extent of any one of these veins; they will be considered along with the arsenopyrite-bearing veins. It should be mentioned here that the Mt. Reid material is remarkably similar to that of the arsenopyrite-bearing veins in mineralogy and textural characteristics. The principal differences being the presence of pyrrhotite in the Idaho Hill-Mt. Folle material, and the absence of tetrahedrite. Also

sphalerite and chalcopyrite are much more abundant in the veins of the Idaho Hill-Mt. Folle area.

The vein material from the Union Mines adit consists essentially of massive coarse-grained arsenopyrite which has been fractured to some extent. Stringers of pyrrhotite, chalcopyrite and pyrite, along with stringers of deep red (almost black) sphalerite are found at the margins of the massive arsenopyrite, penetrating both the host rock and the arsenopyrite. These stringers often connect small clusters or masses of the same sulfides which make up the stringers. The pyrite in these stringers is present as euhedra surrounded by a mixture of pyrrhotite and chalcopyrite. Pyrrhotite is always dominant in these stringers, although this mineral and chalcopyrite do appear to be contemporaneous. The material of the stringers appears to have slightly corroded the arsenopyrite. Galena is present as widely scattered blebs in the arsenopyrite or as isolated grains intergrown with arsenopyrite (Plate. 7). Sphalerite, in addition to occurring in the stringers, is found as blebs in the arsenopyrite and appears to replace this mineral to a limited extent. Quartz and calcite are the only gangue minerals noted in these veins and constitute only a minor proportion of the vein; often composing less than 20% of the vein material. The gangue is medium- to fine-grained, with quartz and calcite being intergrown and showing very little euhedral development. The gangue is usually dominated by quartz, although calcite may be more abundant locally. The veins were reported by previous workers (Cairnes, 1912; Cockfield and Bell, 1944) to be vuggy but no vugs were observed during this study. Vein minerals, both gangue and sulfides, are in direct contact with the host rock with no intervening gouge and little or no alteration; this coupled with the tendency of the veins to pinch and swell erratically (a tendency no longer clear due to limited exposures) led Cairnes (1912) to conclude that these veins were replacing the host rock.

Samples taken from the veins in Schnabel Creek Canyon, as well as from the mountainside between the creek and the Union Mines adit, normally carry a much lower proportion of arsenopyrite and a much higher proportion of the other sulfides, especially pyrrhotite and sphalerite compared with samples in or near the adit. No references to



Plate.7 Arsenopyrite (light gray) from Idaho Hill with galena(darker gray) filling cavities.

Field of view is 1.5mm.

pyrrhotite can be found in the previous descriptions of veins in this area which seems odd in light of its apparent abundance in the veins and the ease with which it may be identified. In some samples pyrrhotite is the dominant sulfide. In all of these samples, arsenopyrite and pyrite appear to be early as they are generally more or less euhedral and somewhat fractured. The other sulfides often fill in these fractures. Sphalerite, again extremely dark, often appears to replace pyrrhotite while both of these are seen to replace galena. Arsenopyrite is also replaced by sphalerite. Chalcopyrite is present as rare inclusions and stringers in the other sulfides. The abundance of gangue increases greatly in these veins relative to material from the Union Mines adit. The gangue normally comprises more than fifty percent of vein material in these samples. Milky, anhedral quartz, which is medium- to fine-grained, is the sole constituent of the gangue. Sulfides mostly occur as stringers and isolated masses filling interstices in the quartz. The vein material mentioned earlier, which had been uncovered in an open cut is an exception in that it exhibits a crude banding. Two bands of sulfides, each with a 1 to 2cm band of quartz at its outer edge, are separated by a central band of quartz 2 to 3cm wide. Within each sulfide band arsenopyrite is always nearest to the quartz essentially forming an envelope filled by the other sulfides which exhibit the textural relationships described above.

### Paragenesis

The paragenesis of the arsenopyrite-bearing veins is characterized by two distinct stages (Fig. 7). The first stage involved the deposition of arsenopyrite and quartz-carbonate gangue. At times the arsenopyrite mineralization is quite massive as seen in the Union Mines adit while in other instances it takes the form of disseminated grains or stringers in the gangue. A variable amount of galena was deposited with this arsenopyrite. The second stage of mineralization is represented by the pyrrhotite-pyrite-chalcopyrite and sphalerite stringers in the adit material. In the Schnabel Creek material, the second stage minerals are seen to fill fractures in the primary arsenopyrite. The replacement textures are more clearly delineated in this material indicating a depositional sequence in which arsenopyrite and galena were laid

## Arsenopyrite-bearing veins

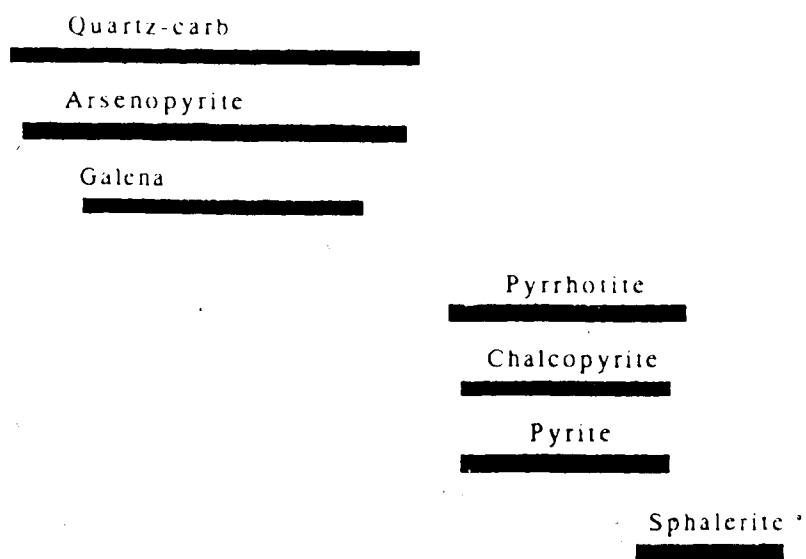


Figure.7 Idealized paragenetic sequence of the arsenopyrite-bearing veins.

down first, followed by pyrrhotite, chalcopyrite and pyrite, with sphalerite occurring last.

## 1. Discussion

Based on the foregoing descriptions, it may be concluded that mineralization on the various showings in the valley was confined to one or two events. Regardless of the number of events mineralization styles are the same in nearly every case, i.e. sulfides are distributed sparsely throughout the gangue as stringers and pods, only occasionally forming massive accumulations. Even though sulfide mineralization is so erratic, deposition almost always progressed sequentially as evidenced by fracture fillings and replacement textures. Descriptions from the literature indicate that precious metal values (especially silver) were always highest when galena was present in the showings. Whether this fact is a simple coincidence or a bona fide genetic indicator remains to be seen.

The timing and age of formation of the various veins cannot be fixed with precision. The three types do not intersect one another in any location nor are widespread marker units present in the valley, which means that relative ages cannot be established. The veins are obviously younger than their host rocks but this fact gives only a minimum age which for most showings is late Cretaceous or early Tertiary based on ages for the Coast Plutonic Complex (LeCouteur and Tempelman-Kluit, 1976; Morrison *et al.*, 1979). Cairnes felt that the galena-bearing veins (gold-silver veins of his study) were possibly late Jurassic in age because of the presence of the basalt dike adjacent to the Mt. Anderson vein. Bull (1986) states that the dike is definitely older than the vein based on the hydrothermal alteration of the dike. This means that a late Jurassic age is not necessarily valid for these veins. Only the stibnite veins of Carbon Hill can be assigned a reliable lower limit to their age because of the rhyolite dike of the Skukum Group which intrudes the shear zone there. The Skukum Group rhyolite plugs have been dated by Pride and Clark (1985) as early Eocene. Suitable material for isotopic dating is not generally present within the veins themselves. Due to this difficulty in establishing either relative or absolute age relationships, it is not possible to unequivocally state whether the various veins are discrete entities or different aspects of a single system. The

fluid inclusion and stable isotope studies described in the following chapters were undertaken to help discern the true relationships among the many different veins.



## V. FLUID INCLUSION STUDY

### A. Introduction

A fluid inclusion study was carried out on vein material from every locality in the study area in order to obtain data on the temperature and pressure of formation of the various veins, as well as, to provide information about parent fluid compositions. Fluid inclusions provide the best means for gathering such information as they are samples of the parent fluid, trapped in the mineral as it grew (Roedder, 1979, Hollister, 1981)

### B. Inclusion Petrography

Doubly polished thick sections were prepared from vein samples from each showing. These sections were then examined for the presence of fluid inclusions using the criteria of Roedder (1984) to determine which inclusions were primary, pseudo-secondary, and secondary. Of the samples examined, quartz proved to be the only mineral which contained usable inclusions in every case, save one. In some instances, the mineral was not clear enough to allow observation (e.g. sphalerite), in others, no primary inclusions could be located (barite and calcite). The one exception was fluorite in a sample of vein material from Mt. Anderson provided by John Biczok. The fluorite did not require polishing; cleavage plates were sufficiently clear to allow microthermometric analysis.

Useable inclusions were not distributed with any degree of regularity in the samples. Inclusions were often found in one sample from a particular locality and not in another, although the samples otherwise would appear identical. Primary inclusions were absent or too small for analysis (less than  $5\mu\text{m}$ ; Roedder, 1984) in several instances, e.g., the massive arsenopyrite veins of Idaho Hill, the Mt. Reid galena-arsenopyrite vein and the second generation quartz of the Carbon Hill stibnite-bearing veins. No useable inclusions were found in any material from Tally-Ho Hill. In the galena-bearing veins of Gold Hill, Mt. Stevens, and Mt. Anderson secondary inclusions were so abundant that primaries were difficult to distinguish except in the vicinity of small, widely scattered vugs.

Inclusions varied considerably from one locality to another and, in some instances, from one sample to another from a single locality. The inclusions may be grouped into three categories based on their appearance at room temperature. The first type (I) consists of, essentially, pure low salinity H<sub>2</sub>O with relatively high liquid/vapor ratios (Volume % liquid is always greater than vapor). In these inclusions, CO<sub>2</sub> is not visible, nor is the presence of CO<sub>2</sub> indicated during freezing runs (Plate 8). The second type (II) includes inclusions that contain a variable amount of CO<sub>2</sub> in addition to H<sub>2</sub>O (Plate 9). The CO<sub>2</sub> may constitute a considerable proportion of the inclusion mass, thereby being readily visible or it may only be indicated by its effects on phase changes during freezing runs. The third type (III) of inclusions is comprised of those inclusions that contain pure or nearly pure CO<sub>2</sub> (Plate 10). These inclusions melt completely at or below the triple point of CO<sub>2</sub> (-56.6°C) and homogenize below the critical point of CO<sub>2</sub> (31.1°C). No daughter minerals were observed in any inclusions examined in this study. Any particular vein of any type might contain more than one category of inclusion.

### C. Techniques and Apparatus

Once suitable inclusions were identified in a chip, the locations of the inclusions were marked on the chip with indelible ink. After this was done, a sketch was made of the inclusion and the maximum dimension of both the inclusion and the vapor bubble were recorded. Microthermometric measurements were then performed on the inclusions using a USGS type heating/cooling stage manufactured by Fluid, Inc. of Denver, Colorado. The stage was mounted on a Leitz microscope fitted with 10x oculars and with 4x, 10x and 32x EF objectives. All measurements were made using the 32x objective. Descriptions of the stage, as well as, operational techniques are found in Woods et al. (1981), Roedder (1984), and Reynolds and Beane (1985). The accuracy of this stage using a SCXIN-O2OU-4.5in thermocouple with a Doric 'Trendicator' temperature readout is quoted as  $\pm 0.1^\circ\text{C}$  in the range -56.6 to +660.4°C by the manufacturer. The apparatus was calibrated using liquid nitrogen, an ice water bath and Merck standard 9800 (melting point 200°C). Temperature



Plate 8. Type I inclusion from Mt. Anderson. Field of view is 0.75mm.



Plate 9 Type II inclusion from Gold Hill; bubble is CO<sub>2</sub>. Field of view is 0.75mm.

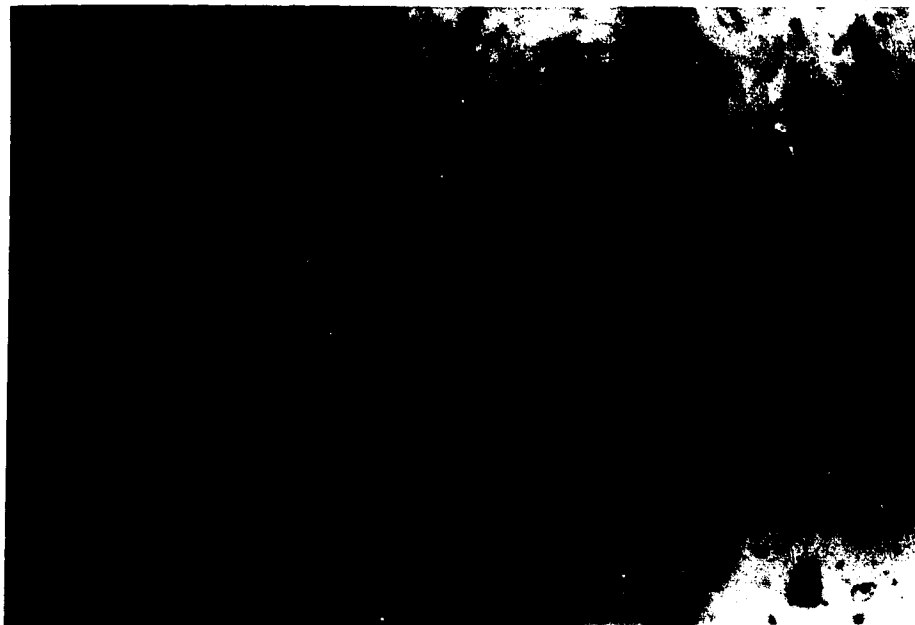


Plate.10 Type III inclusion from Yukon Antimony adit, Carbon Hill. Field of view is 0.75mm.



gradients in the sample are specified as being less than  $0.1^\circ$  at  $-56.6^\circ\text{C}$  and  $-6.6^\circ\text{C}$ ; and less than  $1^\circ$  at  $290^\circ\text{C}$  over an area 5mm in diameter around the tip of the thermocouple (Reynolds and Beane, 1985).

Normally several inclusions were measured in each chip, but any single chip was subjected to only one series of freezing/heating runs. Freezing measurements were performed first, as recommended by Roedder (1984), because of the possibility of stretching of inclusions at high temperatures. All inclusions were cooled to  $\approx 100^\circ$  to  $-110^\circ\text{C}$  to insure that any  $\text{CO}_2$  present was frozen or formed  $\text{CO}_2$ -hydrate. Once all freezing measurements were done, homogenization runs were performed immediately without removing the sample from the stage. If a significant amount of decrepitation occurred during a heating run the chip was normally discarded, especially if previous homogenization temperatures could no longer be duplicated. Three types of homogenization (shrinkage and disappearance of vapor bubble, growth of bubble and disappearance of liquid, and fading of the meniscus) were witnessed during the course of this study, so that homogenization numbers may reflect any of three possible events; this will be discussed further where appropriate.

The data derived from the microthermometric analyses are summarized in Figs. 8-13 (a complete listing of data is provided in Appendix 1). Average values for each analytical category are listed in Table 1. Also provided are the standard deviations from the calculated averages and the number of inclusion analyses upon which the average is based. Any inclusions that were determined to be secondary in origin were not included in the statistical calculations.

#### **D. Low Temperature Measurements**

Low temperature microthermometry produces data of four types:  $\text{CO}_2$  melting temperature ( $T_{m\text{CO}_2}$ ), ice/brine melting temperature ( $T_{m\text{lce}}$ ),  $\text{CO}_2$ -clathrate melting temperature ( $T_{m\text{Clath}}$ ), and  $\text{CO}_2$  homogenization temperature ( $T_{h\text{CO}_2}$ ). The ice melting temperature is a measure of the salinity of the fluid contained in inclusions where  $\text{CO}_2$  or other gases are not present (Potter *et al.*, 1977; Hollister, 1981). Salinity as used here refers to

Table 1 Average values derived from fluid inclusion data, listed by locality (See Appendix I for list of abbreviations).

Sample number	Vol% H <sub>2</sub> O	Vol% CO <sub>2</sub> (l)	Vol% CO <sub>2</sub> (g)	Vol% CO <sub>2</sub> (t)	TmCO <sub>2</sub>	TmIce	Tm Clath	ThCO <sub>2</sub>	Th	Wt% NaCl (fpd)	Wt% NaCl (Clath)
Average(Lm)	77								156.3		
st dev.	10								20.9		
no. of incs.	7								7		
Average(YA)	73	38	62		57.0	3.5		27.2	200.4	5.7	
st dev.	9	13	13		0.4	1.3		3.1	23.7	2.0	
no. of incs.	34	20	20		23	39		22	37	39	
Average(Po)	73	55	45		56.9	2.5		22.5	198.4	4.2	
st dev.	9	11	11		0.2	2.3		2.9	18.2	3.5	
no. of incs.	31	13	13		14	31		14	29	31	
Average(GH)	66			31		2.9	7.8		283.6	4.8	4.3
st dev.	12			11		0.0	1.0		16.9	0.0	1.6
no. of incs.	41			23		2	36		40	2	36
Average(DC)	54	60	40	47	56.8		7.9	29.8	311.2		4.1
st dev.	13			12	0.2		0.3	0.5	18.0		0.6
no. of incs.	19	1	1	13	16		16	2	18		16
Average(MA)	66					3.7			225.9	6.0	
st dev.	7					0.4			16.2	0.6	
no. of incs.	15					15			14	15	
Average(MA9)	84					0.3			186.8	0.6	
st dev.	3					0.1			15.7	0.1	
no. of incs.	25					25			25	25	
Average(MA-fl)	83					0.2			171.4	0.4	
st dev.	3					0.0			3.2	0.1	
no. of incs.	24					24			24	24	
Average(MS)	78			22			8.0		261.0		4.0
st dev.	5			5			0.3		19.8		0.6
no. of incs.	22			22			22		21		22

Note: st. dev.--standard deviation  
All volumes estimated visually.

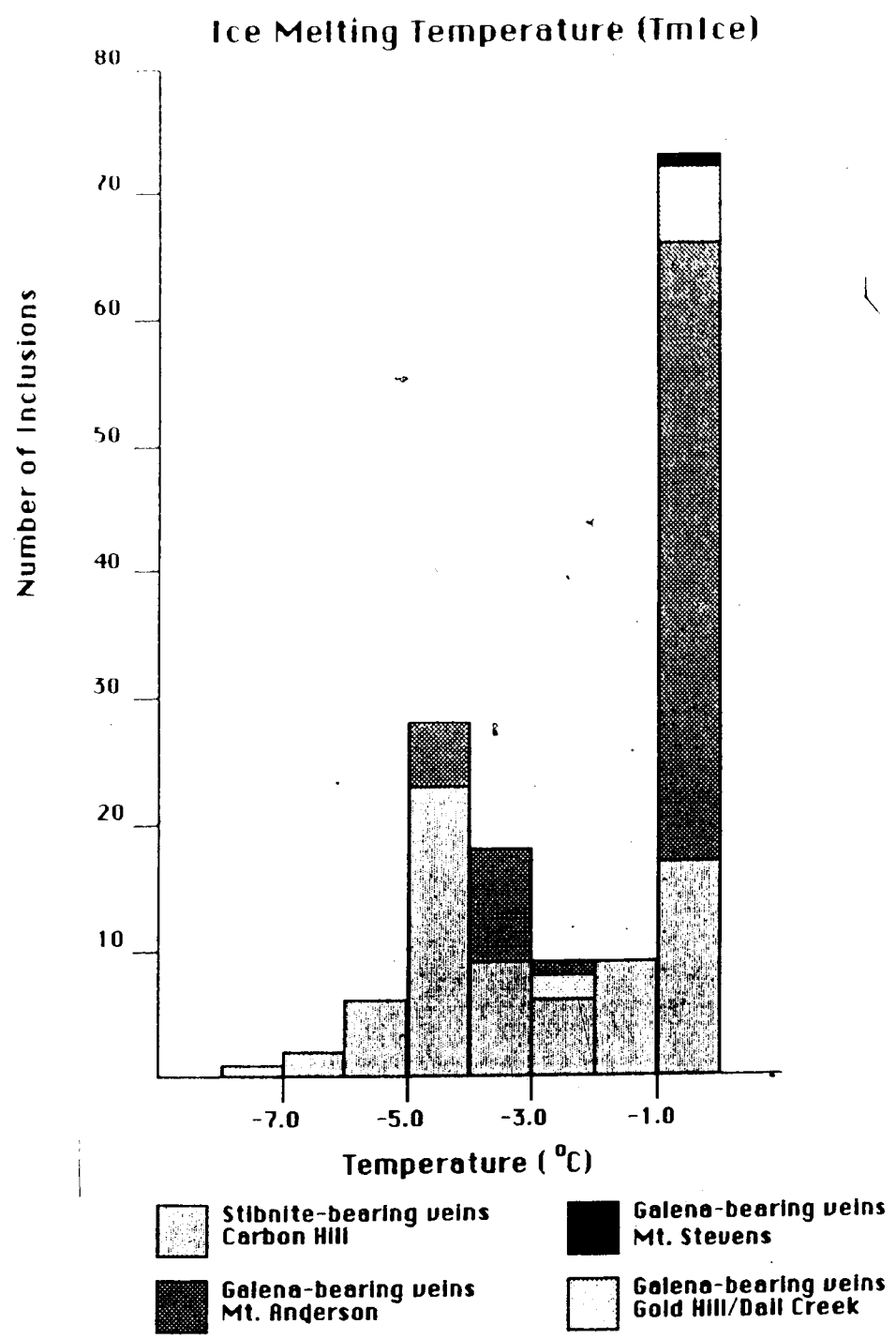


Figure.8 Fluid inclusion ice/brine melting temperatures.



### Clathrate Melting Temperature (TmClath)

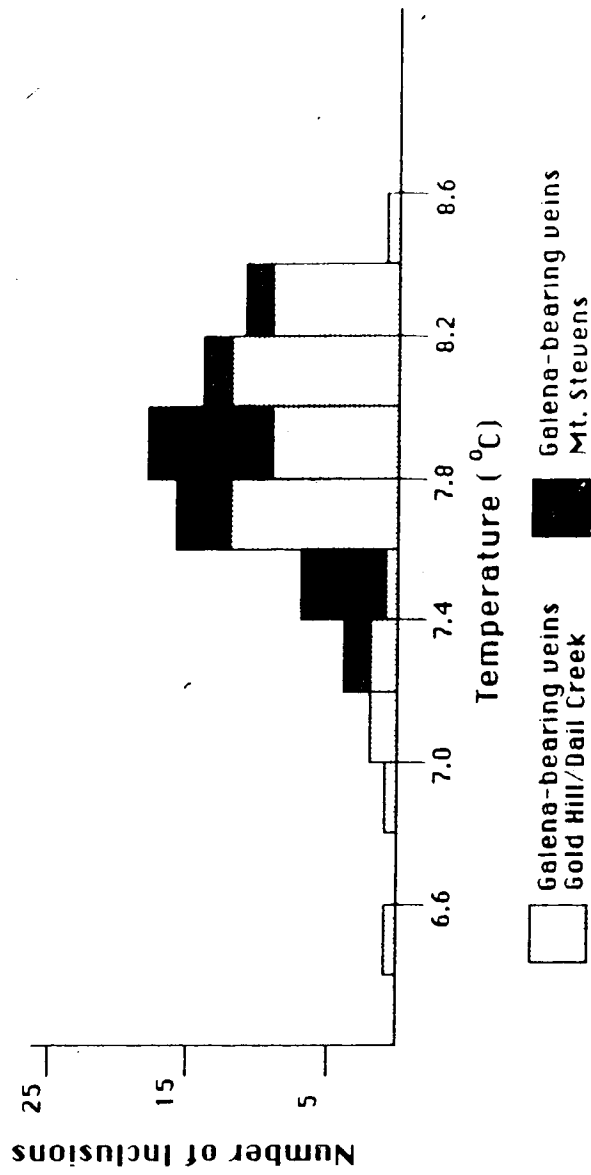


Figure.9 Fluid inclusion CO<sub>2</sub> clathrate melting temperatures.

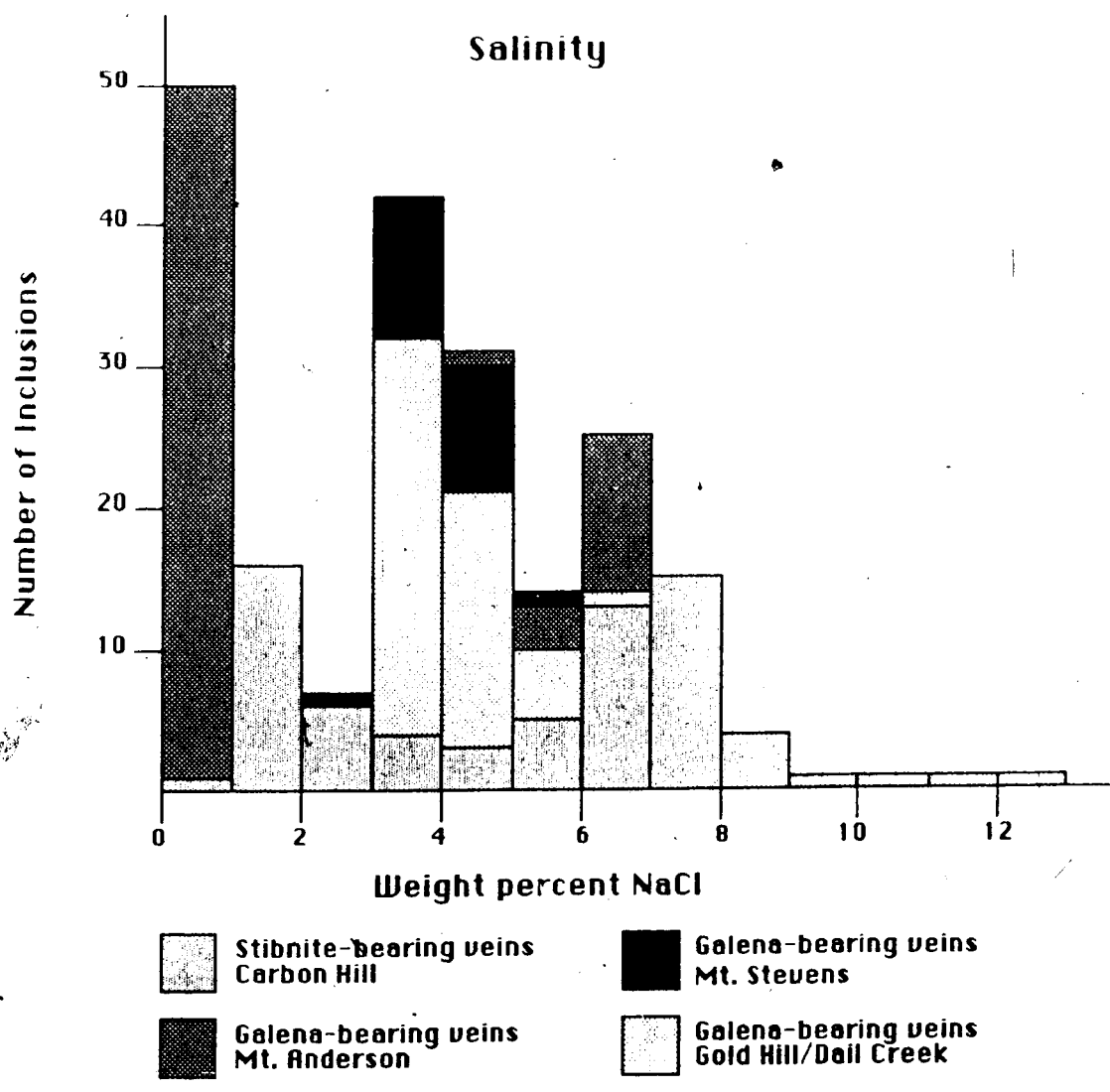


Figure.10 Salinities derived from TmIce and TmClath measurements.

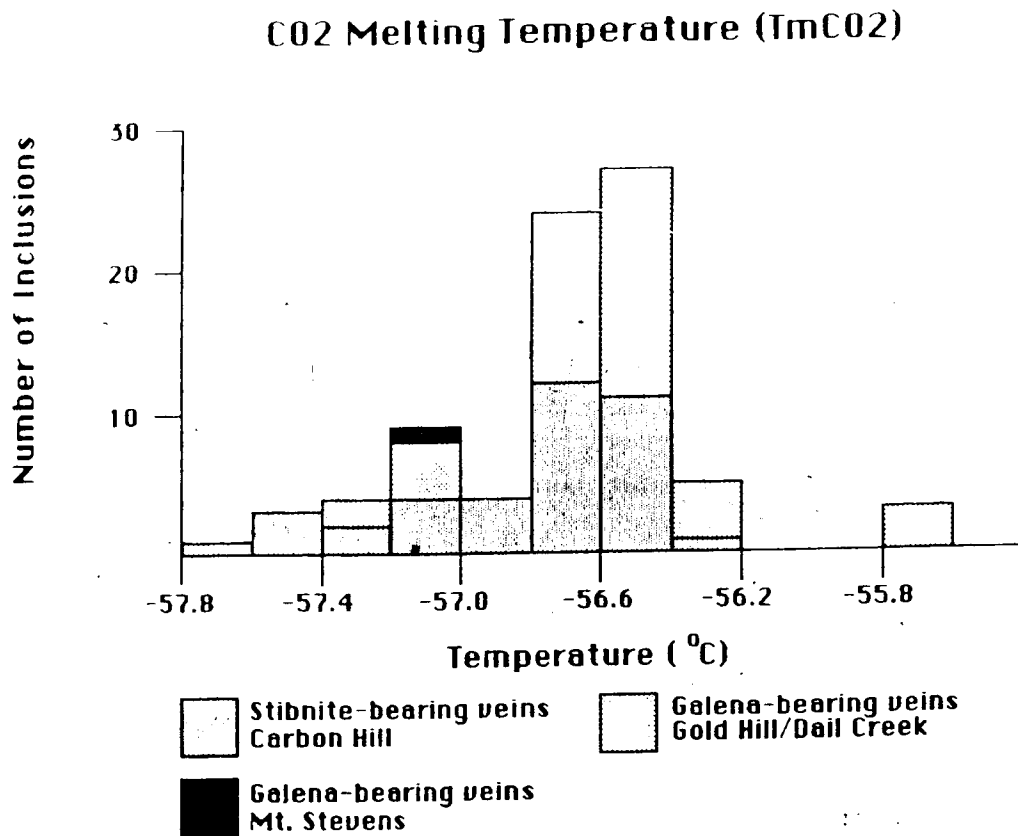


Figure.11 Fluid inclusion CO<sub>2</sub> melting temperatures.

### CO<sub>2</sub> Homogenization Temperature (ThCO<sub>2</sub>)

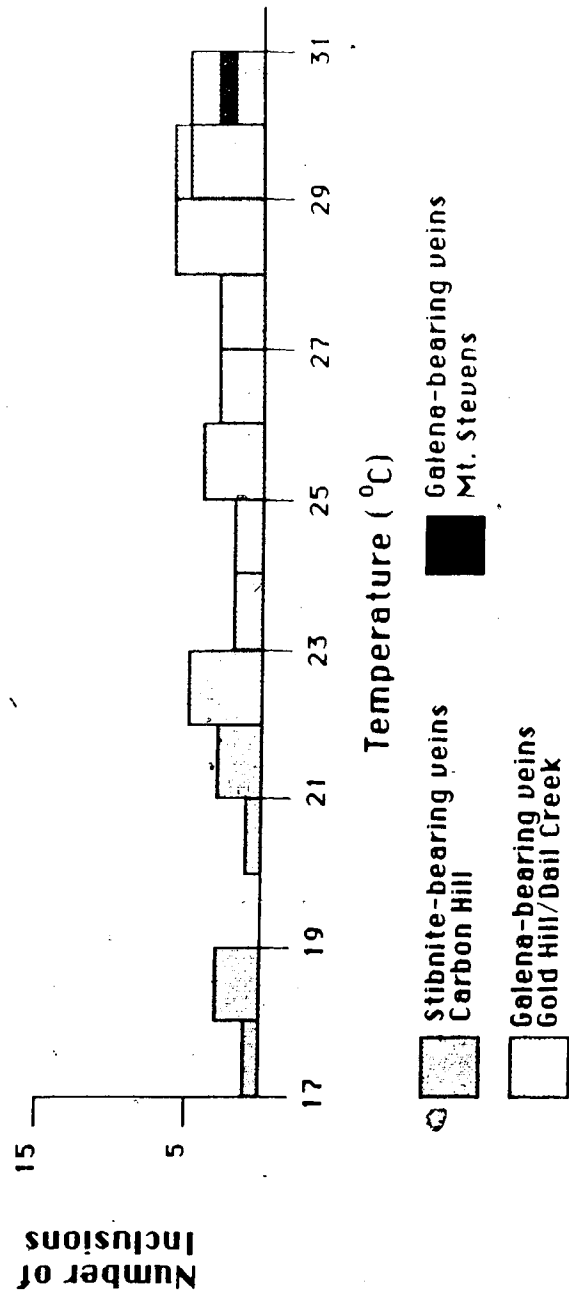


Figure.12 Fluid inclusion CO<sub>2</sub> homogenization temperatures.

# Temperature of Homogenization (T<sub>h</sub>)

All Vein types

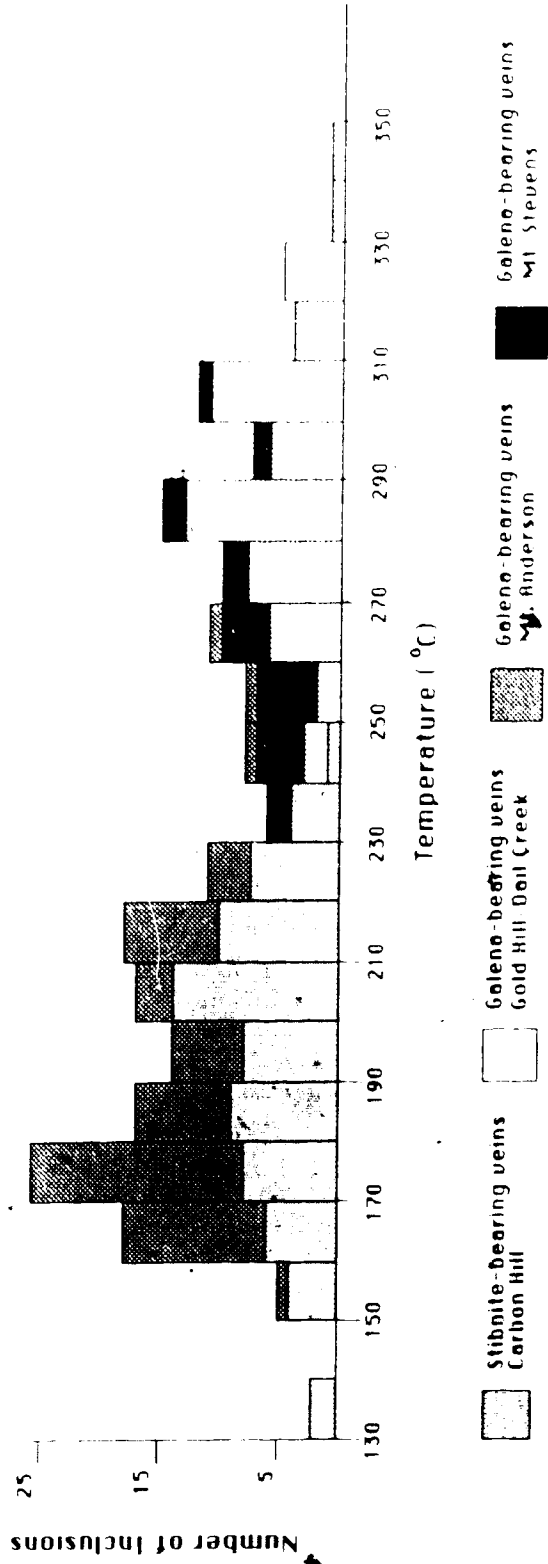


Figure 13 Fluid inclusion homogenization temperatures.

total NaCl equivalent salinity, i.e. the presence of all the common highly soluble salts of  $K^+$ ,  $Ca^{2+}$ ,  $Mg^{2+}$ ,  $Fe^{2+}$ , etc., as well as NaCl. Potter and Clyne (1977) showed that addition of these other salts gave results for total salinity within 1wt % of the NaCl-H<sub>2</sub>O system. This means that determination of the freezing point depression (the amount of lowering of the freezing point of pure H<sub>2</sub>O) will give a very good approximation of total salinity, in wt.% NaCl equivalent, of the parent fluid. Salinity was calculated according to the formula developed by Potter *et al.* (1978), which is

$$W = 0.00 + 1.769581 \times 10^{-4} T^2 + 5.2778 \times 10^{-6} T^3 \quad (\text{Eq. 1})$$

Where  $W$  is wt.% NaCl and  $T$  is freezing point depression in °C. The accuracy of this equation is stated by the authors to be  $\pm 0.028$ wt.% NaCl. The presence of cations other than  $Na^+$  are indicated by their effects on the eutectic temperature in the H<sub>2</sub>O-NaCl system. The eutectic temperature is recognized by the appearance of the first liquid to melt upon warming of the inclusion. Poor optical quality and the small size of the inclusions dealt with in this study prevented the determination of  $T_e$  for any inclusions.

$T_{mIce}$  was determined by observation of inclusions as they were slowly warmed ( $+0.3$  to  $+0.4^\circ\text{C}/\text{min}$ ) near the melting temperature after supercooling, as recommended by Roedder (1984). Supercooling is necessary because of the difficulty in nucleating ice crystals in small inclusions during freezing (Crawford, 1981). In most instances, direct observation of ice formation and melting was not possible; instead, final melting temperature was determined by incremental heating near the melting temperature. In this technique, the inclusion is warmed by small increments,  $0.1$  to  $0.2^\circ\text{C}$ , near the melting temperature until the vapor bubble fails to shrink immediately upon switching off the heating element. Similar methods were employed for  $T_{mClath}$  measurements.

In those inclusions where  $CO_2$  is present in addition to a brine solution, ice melting temperature is no longer an accurate indicator of salinity (Collins, 1979). The reason for this is the formation of the  $CO_2$  clathrate,  $CO_2 \cdot 5.75H_2O$ , during freezing. The formation of the

clathrate subtracts large quantities of H<sub>2</sub>O from the solution, thereby making the apparent salinity of the depleted fluid much greater than the true value. Collins (1979) has shown that the final melting temperature of the clathrate varies systematically with the salinity of the fluid. T<sub>m</sub>Clath is depressed as salinity increases, much like the freezing point of pure water. Therefore, it is possible to obtain a good approximation of true salinity based on T<sub>m</sub>Clath, by using the formula given by Bozzo *et al.* (1975)

$$W = 15.52023 + 1.02342T - 0.05286T^2 \quad (\text{Eq. 2})$$

Where W is wt % NaCl and T is T<sub>m</sub>Clath

The melting temperature of CO<sub>2</sub> (-56.6°C) is used to determine the purity of this phase. If the phase melts at any lower temperature, then the presence of another gaseous phase is indicated, e.g. CH<sub>4</sub> or, less commonly N<sub>2</sub> (Burruss, 1981). CH<sub>4</sub> is by far the most common gas found associated with CO<sub>2</sub> in fluid inclusions (Roedder, 1984). Since CH<sub>4</sub> and NaCl have opposing effects on T<sub>m</sub>Clath measurements, it is essential that the CH<sub>4</sub> content be estimated in order to determine the validity of salinity calculations based on T<sub>m</sub>Clath. Two methods were used in this study to estimate CH<sub>4</sub> content. The first, described by Swanenberg (1979), is a graphical method of determining mole fraction CH<sub>4</sub> using T<sub>m</sub>CO<sub>2</sub> and degree of fill at T<sub>m</sub>CO<sub>2</sub>. This method worked quite well for type III inclusions. The second method, presented by Burruss (1981b), involves the use of T<sub>m</sub>CO<sub>2</sub>, T<sub>h</sub>CO<sub>2</sub> and homogenization phase with known P-V-T-X data to calculate CH<sub>4</sub> content. This method was limited in its usefulness due to the lack of T<sub>h</sub>CO<sub>2</sub> data (because of poor visibility) for those inclusions for which it would have been most appropriate (type II).

T<sub>m</sub>CO<sub>2</sub> was more difficult to measure than any other parameter. The difficulty arose due to the rapidity with which the phase change occurred and the tendency of the apparatus to warm up too quickly at very low temperatures. A further complication was poor visibility in many type II inclusions. Because of these difficulties, T<sub>m</sub>CO<sub>2</sub> values were generally checked several times to improve accuracy. T<sub>h</sub>CO<sub>2</sub> was impossible to determine in many type II

inclusions because of poor visibility. In those inclusions where it could be determined (especially type III) cycling was employed to fix  $\text{ThCO}_2$  as precisely as possible.

#### E. High Temperature Measurements

High temperature measurements in this study were confined to homogenization temperatures ( $T_h$ ). No attempt was made to systematically determine decrepitation temperatures, as they provide little useful information (Roedder, 1984). As was stated earlier, if decrepitation was suspected in any inclusion it was ignored and if widespread decrepitation was seen the chip was discarded.  $T_h$  values for a fluid define an isochore (or line of constant molar volume) for that fluid. If the P-V-T-X properties for that fluid are known, then fluid compositions can be calculated using  $T_h$  data. If pressure at the time of trapping ( $P_t$ ) is known or can be estimated, then trapping temperature ( $T_t$ ) can be determined from this isochore (Hollister, 1981).

#### F. Discussion of Results

##### Stibnite-bearing Veins

Fluid inclusion analyses served to reinforce indications that the stibnite-bearing veins which occur in the Yukon Antimony and Porter adits on Carbon Hill are closely related. Both showings contained type I and III inclusions, which were usually closely associated within a sample. Averages for all analytical categories are very similar. The  $\text{ThCO}_2$  averages are the farthest apart in absolute terms but even these two numbers are actually very close when standard deviations are considered. High and low values are also very similar in each category. Salinities of the type I inclusions reflect the difference in  $T_{m\text{Ice}}$  averages for the two showings, being 5.7 and 4.2 wt.% eq. NaCl for YA and Po, respectively.

The close association of type I and III inclusions in the vein material from these showings indicates that the inclusions are contemporaneous. If the two types are contemporaneous, then this suggests that  $\text{CO}_2$  effervescence occurred throughout the system.



This in turn means that a unique  $P_t$  and  $T_t$  may be fixed for the system, because an effervescing system is at its vapor pressure, meaning no correction for depth need be made. The  $P_t$  and  $T_t$  are given by determination of the intersection of the isochores for the two fluids after plotting the isochores (using the data of Angus *et al.* (1976), and Sourirajan and Kennedy (1962)) on a common  $P-T$  plot (Kalyuzhnyi and Koltun, 1953; Roedder and Bodnar, 1980). Construction of such isochores gives a  $P_t$  value of approximately 1180 bars and a  $T_t$  of 230°C. A relatively minor error in constructing the isochores or in determining the homogenization temperatures will result in an error of several tens of bars for  $P_t$  and a similar error for  $T_t$ . For this reason, the values given above should be considered representative of ranges for  $P_t$  and  $T_t$ , respectively. Ramboz *et al.* (1982) question the validity of this method, but suggest that it may still provide a rough guide for  $P_t$  and  $T_t$ .

Using Swanenbergs' (1979) method with the type III inclusions showed that the  $CH_4$  content was less than 0.05 mole % in almost every case which means these fluids can be considered essentially pure  $CO_2$ . The average  $T_hCO_2$  values for Yukon Antimony and Porter Claims samples are 21.2° and 22.5°C respectively, which correspond to fluid densities in the range 0.85 to 0.75g/cm<sup>3</sup>, based on the  $P-T$  diagram of Angus *et al.* (1973).

A total of only seven useable inclusions could be located in the Em stibnite-bearing vein material. Optical properties of these inclusions were so poor that only  $T_h$  data could be obtained, meaning that the composition of the fluid in them can not be determined with any degree of confidence.

### **Galena-bearing Veins**

The galena-bearing veins show a great deal of variation in one category, but are remarkably similar in two others. The average homogenization temperatures vary from a high of 311°C in the Dail Creek vein to 226°C in the Mt. Anderson vein, with the Gold Hill and Mt. Stevens averages being 284° and 261°C, respectively.  $T_mClath$  data determined for Dail Creek, Gold Hill, and Mt. Stevens varied by only 0.2°C from the high of 8.0°C (MS) to the low of 7.8°C (GH). These similar averages for  $T_mClath$  naturally lead to similar salinities for

the three veins, i.e. 4.1(DC), 4.3(GH), and 4.0wt.% eq. NaCl (MS). Inclusions in the Mt. Anderson vein show no visible indication of the presence of CO<sub>2</sub>; however, Hedenquist and Henley (1985) have shown that even invisible amounts of CO<sub>2</sub> may contribute as much as 1.5°C to the freezing point depression of the fluid. This means that the 6.0wt.% eq. NaCl value for salinity for this vein may be too high by nearly 2wt.% eq. NaCl. If this is true then all of the galena bearing veins would have nearly identical salinity values.

Data in other categories are spotty so that valid comparisons among all four veins can not be made. Only the Dail Creek samples were sufficiently clear so that T<sub>m</sub>CO<sub>2</sub> measurements could be made, but of the 16 inclusions observed only two provided ThCO<sub>2</sub> data. Many of these inclusions exhibited critical behavior during homogenization or homogenized to a gas. This combined with the highly variable phase ratios suggests that the system may have been near the solvus for this composition (Roedder, 1984). If this is true, the homogenization temperature defines a maximum trapping pressure for this showing (Roedder, 1984; Pichavant *et al.*, 1982). In such a case, extrapolating the data of Takenouchi and Kennedy (1965); and Gehrig *et al.* (1979) indicates a likely P<sub>t</sub> of less than 500 bars.

### Other veins

As was mentioned earlier, no useable inclusions could be found in the arsenopyrite veins. A few inclusions were located which appeared to homogenize at approximately 270° to 320°C, but values could not be reproduced. In addition, optical quality was so poor that phase changes at low temperatures could not be discerned.

The chalcedony vein on Mt. Anderson produced many usable inclusions from both the acicular quartz and the fluorite in the vein. No CO<sub>2</sub> was observed in either type of material. Low T<sub>m</sub>ice, Th and salinity values are similar for both materials, but they are much lower than any of the other veins. Salinity is so low that Th values may be applied to the pure H<sub>2</sub>O phase diagram (Fisher, 1976) quite readily with little loss of accuracy. This gives a density for the fluids of between 0.85 and 0.90g/cm<sup>3</sup>. A minimum depth of deposition may be estimated for this vein using the data of Haas (1971). The calculated depth to the boiling surface of

such a dilute fluid is less than 100m.

## VI. OXYGEN ISOTOPE STUDY

### A. Introduction

In order to delineate probable origins and relationships among veins, oxygen isotope data were obtained from all of the showings examined in this study. These data, when used in conjunction with mineralogical determinations and fluid inclusion analyses, provide a basis for making reasonable postulations as to the source and characteristics of the fluid (or fluids) which was responsible for depositing the vein material in each case.

As only a single generation of quartz is present in nearly every case, samples for isotopic analysis were chosen from those specimens in which quartz appeared to be most nearly contemporaneous with sulfide mineralization. If contemporaneity was questionable samples were chosen in which quartz was most intimately associated with the sulfides in the belief that this quartz was most likely to represent material which formed at the same time as the sulfides.

### B. Techniques

After suitable samples were selected, they were crushed to the appropriate fineness, then treated with concentrated acids and/or aqua regia to remove soluble minerals. Heavy liquid separation was employed on those samples in which barite constituted a relatively large proportion of the vein material. Finally, Fe-oxides and other resistant grains were removed by hand-picking of the cleaned and dried sample.

Analysis of the samples was carried out by Dr. Karlis Muehlenbachs in his laboratory using the bromine pentafluoride extraction technique originally described by Clayton and Mayeda (1963). In this technique, the quartz sample is reacted with  $\text{BrF}_3$  in order to liberate  $\text{O}_2$  (possibly according to this reaction:  $\text{SiO}_2 + 2\text{BrF}_3 = \text{SiF}_4 + 2\text{BrF}_2 + \text{O}_2$ ). The  $\text{O}_2$ , thus liberated, is passed over hot carbon to produce  $\text{CO}_2$ , which is in turn frozen out of the product gas by means of a liquid nitrogen trap. The  $\text{CO}_2$  is subsequently analysed in a mass spectrometer to determine the amount of  $^{18}\text{O}$  present relative to a standard. The mass

spectrometer used in the analyses for this study was a Nier type, 90°-sector, double-collecting Micromass 602D. Results are reported in  $\delta$  notation relative to Standard Mean Ocean Water (SMOW) (Craig, 1961). The fractionation factor for  $\text{CO}_2$ - $\text{H}_2\text{O}$  used to calculate results was 1.0412. Analytical error for this laboratory, when employing the above method, is generally reported as  $\pm 0.1\text{‰}$ .

### C. Results of Analyses

Oxygen isotope data from the above analyses are listed in Table 2. Vein mineralogy is also provided for each sample. The data exhibit a range in values which varies from a  $+21.6\text{‰}$  enrichment relative to SMOW to a  $-2.3\text{‰}$  depletion. cursory examination of the data reveals that three distinct groups of  $^{18}\text{O}$  values are present. The first group is a set of extremely  $^{18}\text{O}$  enriched samples from the stibnite-bearing veins of Carbon Hill (CH13, Po14, Fm2, YA18) with values from  $+17.4\text{‰}$  to  $+21.6\text{‰}$ . The second group includes all of the samples of coarse-grained quartz from the galena- and arsenopyrite-bearing veins which show a more moderate degree of  $^{18}\text{O}$  enrichment. The  $\delta^{18}\text{O}$  values for these samples range from  $+6.5\text{‰}$  to  $+12.7\text{‰}$ . The  $+6.5\text{‰}$  value seems to be anomalous as no other analysis is found within approximately  $\pm 3\text{‰}$  of it. If this value is ignored the range for the second group values becomes much narrower, i.e.,  $+9.4\text{‰}$  to  $+12.7\text{‰}$ . The last group of values has a range of  $-2.3\text{‰}$  to  $+1.6\text{‰}$ . Four of the five values in this group come from fine-grained quartz or chalcedony samples taken from Mt. Anderson (MA9, T2-1, T2-3) and Tally-Ho Hill (TH17). The fifth value is from a sample of vein material (Po15) from the Porter adit on Carbon Hill. It is felt that this sample may have been dominated by the second stage quartz identified at this locality, but this could not be confirmed. If, indeed, this was the case, then fine-grained quartz or chalcedony accounts for every instance of isotopically light samples.

Table.2 Results of oxygen isotope analyses (See Appendix I for list of abbreviations)

Sample number	$\delta(18)O$ quartz(‰)	$\delta(18)O$ fluid(‰)	Temp °C	Vein mineralogy
<b>Normal veins</b>				
CH13	21.6	10.0	200.0	qtz-bar-cal-stib (sp-py)
		6.8	160.0	
Po14	17.6	6.0	200.0	qtz-bar-stib-sp-james
Em2	20.0	5.1	156.0	qtz-bar-stib-sp
YA18	17.4	5.8	200.0	qtz-bar-cal-stib-sp-py
MS3	12.7	4.3	261.0	qtz-gn-py-cp-sp
MS10	11.6	3.2	261.0	qtz-gn-py-cp-sp
MS15	12.3	3.9	261.0	qtz-gn
GH1	9.6	2.2	284.0	qtz-py
DC1	10.9	4.4	311.0	qtz-py
MR10	10.7	0.6	230.0	qtz-asp-py-gn (sp)
		2.3	260.0	
		4.2	310.0	
IH7	12.1	5.2	300.0	qtz-asp-po-sp-py-gn
IH18	10.4	3.6	300.0	qtz-asp-po-sp-py-gn-py-(cp)
<b>Low (18)OH2O veins</b>				
MA5	9.4	-0.7	226.0	qtz-ks-cal-gn-sp-py
TH4	6.5	-3.6	230.0	qtz
		-1.9	260.0	
		0.0	310.0	
<b>Chalcedony veins</b>				
MA9	-2.3	-14.8	187.0	qtz-chal
T2-1	-1.5	-15.2	170.0	chal-fl
		-16.8	150.0	
		-18.7	130.0	
T2-3	-1.9	-15.6	170.0	chal-fl
		-17.2	150.0	
		-19.1	130.0	
Th17	-1.0	-14.7	170.0	chal
		-16.3	150.0	
		-18.2	130.0	
Po15	1.6	-9.9	200.0	qtz-gn
		-13.3	160.0	

#### D. Fluid Calculations

Calculated probable  $\delta^{18}\text{O}$  compositions of the parent fluid (or fluids) for each of the veins for which data were obtained provide evidence concerning the source and/or evolution of these fluids. The calculations are performed using the quartz-H<sub>2</sub>O fractionation equation developed by Matsuhisa, et al. (1979), which is as follows:

$$1000 \ln \alpha = 3.34(10^6/T^2) - 3.31 \quad (\text{Eq. 3})$$

where 'T' is the temperature of formation in °K, in this case derived from the average homogenization temperature for each vein taken from the fluid inclusion study described in Chapter V. Using this equation allows the actual calculation of the probable  $\delta^{18}\text{O}$  content of the parent fluid from the relation:

$$1000 \ln \alpha = \delta^{18}\text{O}_{\text{QIZ}} - \delta^{18}\text{O}_{\text{H}_2\text{O}} \quad (\text{Eq. 4})$$

where  $\delta^{18}\text{O}_{\text{QIZ}}$  has been determined analytically (Table 2). The results of the calculations are listed in Table 2. For reasons explained in the previous chapter fluid inclusion data could not be obtained for some specimens therefore several  $\delta^{18}\text{O}_{\text{H}_2\text{O}}$  values (calculated using various temperatures) are listed for some samples. These values were obtained using inferred temperatures of formation. The reasoning behind the choice of temperatures in each case will be explained in the following discussion.

The errors inherent in calculating  $\delta^{18}\text{O}_{\text{H}_2\text{O}}$  values, which are derived from both the  $\delta^{18}\text{O}$  analyses and the Th measurements, mean that any particular  $\delta^{18}\text{O}_{\text{H}_2\text{O}}$  value is only accurate to approximately  $\pm 1\%$ . For example, an error of  $\pm 10^\circ\text{C}$  in the Th used will result in an error of nearly 1% in the calculated  $\delta^{18}\text{O}_{\text{H}_2\text{O}}$  value.

## E. Discussion of Results

### Normal Fluids

For the most part,  $\delta^{18}\text{O}$  values of the ore fluids fall in the range  $+2.2\text{‰}$  to  $+6.8\text{‰}$ . The CH13 sample gives the highest values of  $+10.0\text{‰}$  and  $+6.8\text{‰}$ , but these values are based on temperatures from other showings on Carbon Hill, since no usable fluid inclusions could be found in CH13, itself, or in associated samples. Due to the uncertainty in the true temperature value, the lower figure will be used subsequently in this paper. This  $\delta^{18}\text{O}_{\text{H}_2\text{O}}$  range appears to be continuous for all vein types, but as can be seen in Table 2, no galena-bearing vein has a reliable  $\delta^{18}\text{O}_{\text{H}_2\text{O}}$  value greater than  $+4.4\text{‰}$ , while no stibnite-bearing vein has a value less than  $+5.1\text{‰}$ . The  $0.7\text{‰}$  gap between these two numbers is rather small, possibly insignificantly so, in light of the numerous sources of error and the many approximations that are inherent when combining fluid inclusion and stable isotope data. However, when the averages of the  $\delta^{18}\text{O}_{\text{H}_2\text{O}}$  values for these two groups are compared a difference of  $2.3\text{‰}$  is seen, i.e.,  $+3.6\text{‰}$  vs  $+5.9\text{‰}$ , a difference which may be significant. Since no fluid inclusion data could be obtained from the Mt. Reid (MR) samples,  $\delta^{18}\text{O}_{\text{H}_2\text{O}}$  values were calculated using temperatures derived from other galena-bearing veins. Values for the arsenopyrite-bearing veins are highly speculative, being based on only a few non-repeatable Th values; therefore they were not included in the above comparison. If these data are included, the difference becomes  $2.1\text{‰}$  and the lower average,  $+3.8\text{‰}$ .

### Depleted Fluids

As mentioned earlier, several samples produced  $\delta^{18}\text{O}_{\text{H}_2\text{O}}$  values which do not fall in the range mentioned above, all being lighter than the other samples. These samples come from Mt. Anderson (MA5, MA9, T2-1, T2-3), Tally-Ho Hill (TH4, TH17) and the Porter adit of Carbon Hill (Po15). For the majority of these samples (T2-1, T2-3, TH4, TH17, Po15) no fluid inclusion data could be obtained either due to a lack of suitable inclusions or to the extremely fine grain size of the sample material. While usable inclusions were found in sample



Pol5, these inclusions were present only in the coarse-grained first generation quartz, not in the fine-grained second generation material which made-up an unknown proportion of the sample on which  $\delta^{18}\text{O}$  analysis was performed. Calculated  $\delta^{18}\text{O}_{\text{H}_2\text{O}}$  values for these samples are all highly depleted when compared with the other group of values discussed above. Only one value (TH4) is greater than zero, but this is the result of an hypothetical formation temperature that is probably too high.

#### Mt. Anderson

Two of the Mt. Anderson samples (MA5, MA9) provided sufficient fluid inclusion data so that direct calculation of the  $\delta^{18}\text{O}_{\text{H}_2\text{O}}$  values for these samples was possible. On the other hand, samples T2-1 and T2-3, which were composed of chalcedony contained no usable inclusions. Thus, indirect calculations were made using three different possible formation temperatures for these latter two samples. The highest temperature chosen (170°C) was the approximate temperature of formation derived from the fluid inclusion data of fluorite samples from this locality provided by John Biczok of Noranda Exploration Company, Ltd. This fluorite is intergrown with and is being replaced by the chalcedony in the sample provided. Radial clusters of acicular quartz crystals in contact with chalcedony are also present in this sample, but this type quartz yielded temperatures of homogenization which averaged over 185°C in similar material from sample MA9. This temperature is higher than the 180°C maximum formation temperature for chalcedony given by Fournier(1985), therefore the 170°C temperature derived from the fluorite samples was deemed more reasonable as a maximum formation temperature in this case. In recognition of the fact that the parent fluid could well have deposited the chalcedony at a much lower temperature, the calculations were performed for 150°C and 130°C for comparison purposes.

#### Tally-Ho Hill

Formation temperatures are even more speculative for the Tally-Ho Hill samples (TH4; TH17) as no suitable fluid inclusions could be located in any material from this

showing. Due to this deficiency of data,  $\delta^{18}\text{O}_{\text{H}_2\text{O}}$  values for the two samples were calculated using temperature data from other veins in the valley which appear to have mineralogical and/or textural affinities with these samples. For the coarse-grained material (TH4) 220°, 260° and 310°C were chosen since these temperatures represent the range seen in average homogenization temperatures for galena-bearing veins. Because of the chalcidonic nature of the material in the second sample (TH17) the same temperatures were used in the calculation of possible  $\delta^{18}\text{O}_{\text{H}_2\text{O}}$  values for this sample as were used in the calculations for T2-1 and T2-3 from Mt. Anderson.

#### Carbon Hill

The case of sample Po15 is the most enigmatic of all because of the astonishingly low enrichment of this quartz in  $^{18}\text{O}$ , relative to other samples from Carbon Hill. As discussed in Chapter V, fluid inclusion evidence suggests that the first generation quartz in the Porter adit showing is probably contemporaneous with the quartz of the Yukon Antimony vein, but the affinity of the second generation material is unclear. To use a formation temperature of  $\approx 200^\circ\text{C}$  in the calculation of  $\delta^{18}\text{O}_{\text{H}_2\text{O}}$  for Po15 based on the relationship suggested above does not seem logical for this low  $\delta^{18}\text{O}$  quartz. There is no indication that the much cooler temperature ( $157^\circ\text{C}$ ) derived from the Goddell's Claims (Em) samples is any more appropriate; however, for lack of any better data, 200° and 160°C were used merely to give an indication of the possible  $\delta^{18}\text{O}$  composition of the parent fluid.

#### Present Day Meteoric Water

Present day meteoric water in the southern Yukon has  $\delta^{18}\text{O}$  values in the range of  $-22.5\text{‰}$  to  $-17.5\text{‰}$  and  $\delta\text{D}$  values of  $-170\text{‰}$  to  $-130\text{‰}$  (Sheppard, 1986; Taylor, 1979; etc.). These values are based on the systematic variation of the  $^{18}\text{O}$  and D content of meteoric waters with latitude and elevation; as one or both of these parameters increases so too does the magnitude of the depletion of both  $^{18}\text{O}$  and D (Craig, 1961). Dagenais (1984) reports a  $\delta^{18}\text{O}$  value of  $-21.4\text{‰}$  for a well water sample from the Dezadeash map area which adjoins

the study area immediately to the west. The present day meteoric water line is shown in Fig. 24 with the data from the present study, as well as, data from other deposits or deposit types for comparison. Data for Cassiar and Mt. Skukum are from Nesbitt *et al.* (1986), that for Montana Mountain is from Walton (1987) and that for volcanic epithermal systems is from B. F. Taylor (1987).

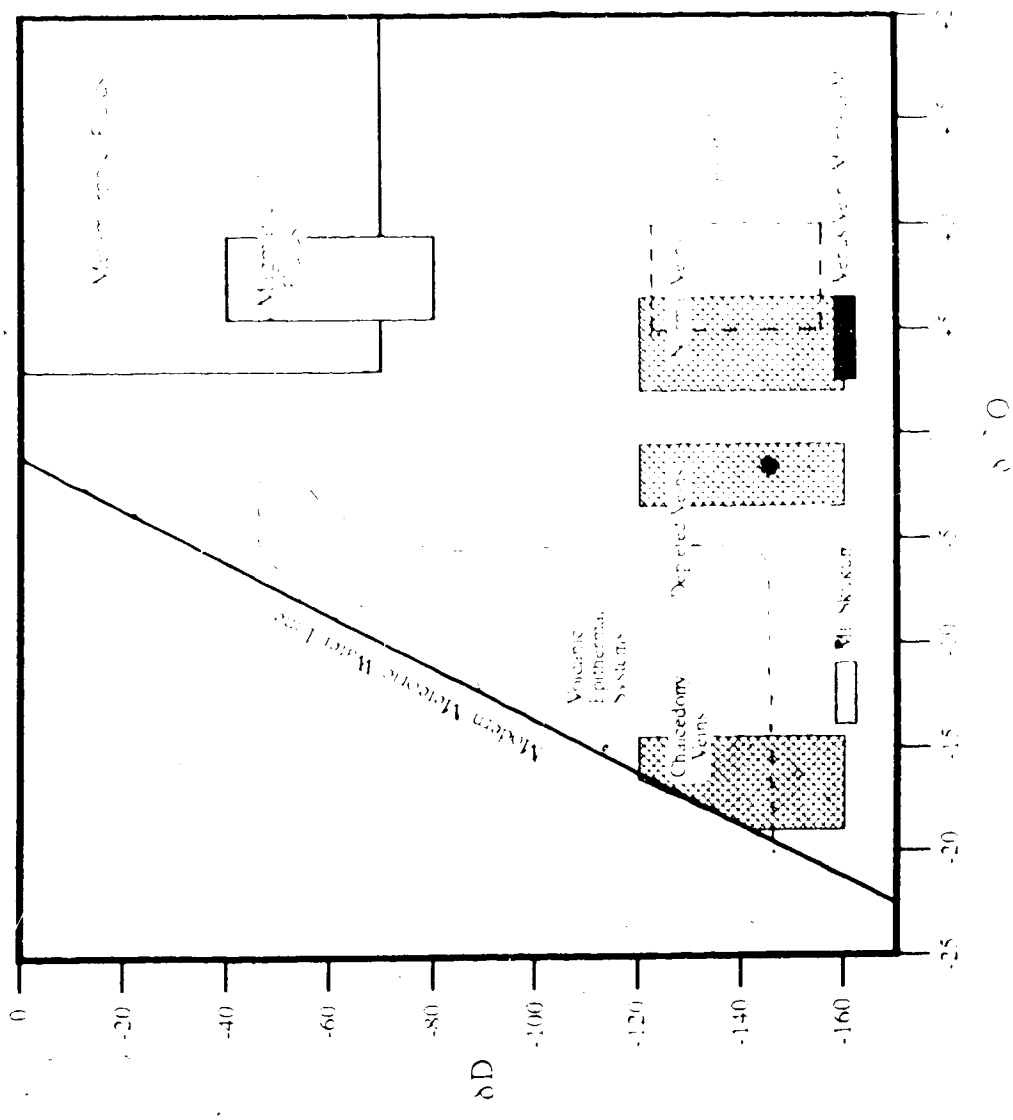


Figure 14  $\delta^{18}O$  versus  $\delta D$  plot showing data from this study in relation to other deposits. Upper 5D data from Magellan, 1987, and lower from Walton, 1987.

## VII. DISCUSSION AND CONCLUSIONS

### A. Introduction

The petrologic, fluid inclusion and oxygen isotope data, when considered together, indicate that the Wheaton River vein system is more complex than first imagined by the author (Fig. 15). These data also serve to point out that more work must be done in the valley by future workers before many questions will be definitively answered. With the data at hand, however, it is possible to make some reasonable postulations as to the genesis and relationships among the various veins.

Current consensus (Sheppard, 1986; Taylor, 1979) seems to indicate that the meteoric water line has remained essentially constant throughout much of the Phanerozoic (especially the Mesozoic and Cenozoic) with minor shifts being likely over time, but at all times possessing the same slope. However, this obviously does not mean that  $\delta^{18}\text{O}$  and  $\delta\text{D}$  values of meteoric waters for any particular geographic area have not changed through time. Tectonic movements will cause both latitudinal and elevational changes as plates shift over the earth's surface. Changing climatic conditions (wind direction, humidity, etc.) will also have considerable effects on stable isotope variations (H.P. Taylor, 1979).

As the deposits of the Wheaton River valley are all Cretaceous or younger in age, some estimate of the stable isotope content of the meteoric waters of this time period is necessary in order to make valid comparisons. Dagenais (1984) has concluded that  $-16\text{‰}$  is a reasonable value for the  $\delta^{18}\text{O}$  content of meteoric water in the Whitehorse Trough during Cretaceous and Tertiary times. Data obtained from their Skagway-Carcross traverse led Magaritz and Taylor (1976) to calculate a value of  $-120\text{‰}$  for  $\delta\text{D}$  of meteoric fluids in this area during the early Tertiary. Walton (1987) reports a  $\delta\text{D}$  value of  $-159\text{‰}$  for a sample from the Venus Vein on Montana Mountain. These two values are used as the upper and lower limits for  $\delta\text{D}$  of fluids in this study plotted on Fig. 14.

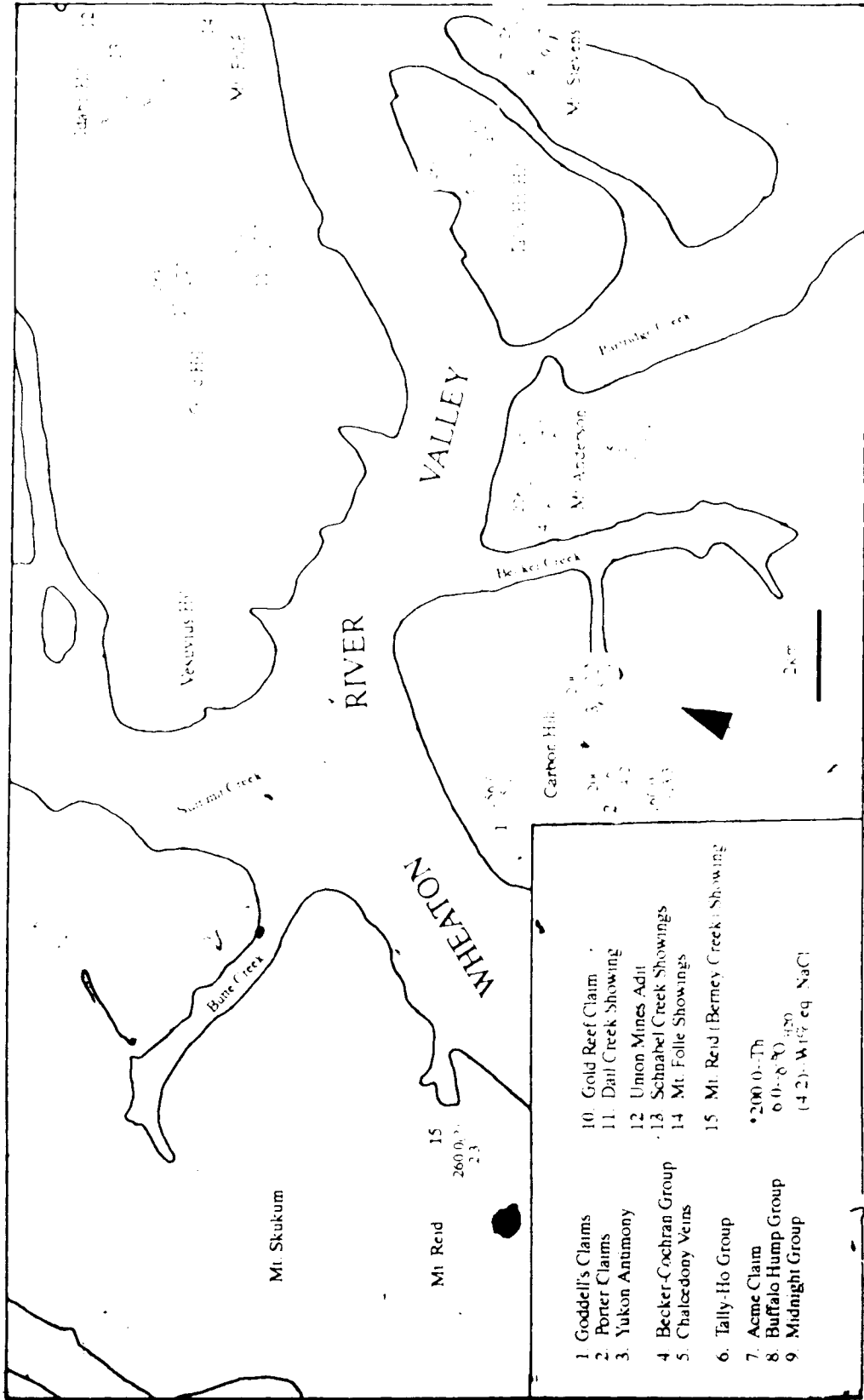


Figure.15 Map showing the distribution of isotopic and fluid inclusion data in the study area.

## B. Models for Vein Deposition

### Galena-bearing Veins

#### Meteoric Derivation

The isotopic values for the galena-bearing veins may be explained by three parent fluid derivation models. Calculated  $\delta^{18}\text{O}_{\text{H}_2\text{O}}$  data for these veins, on the whole, show a considerable enrichment in  $^{18}\text{O}$  relative to the assumed  $-16\text{‰}$  value for pristine meteoric water. The enrichment is on the order of  $+20\text{‰}$  for galena-bearing veins (assuming an average  $\delta^{18}\text{O}_{\text{H}_2\text{O}}$  value of  $+3.6\text{‰}$ ). The enrichment in  $^{18}\text{O}$ , which the fluids for most of the principal showings exhibit, indicates considerable water/rock-interaction. This enrichment of  $^{18}\text{O}$  "shift" has been noted in many modern geothermal areas (Craig, 1963; Taylor, 1979; Field and Fifarek, 1985; etc.). In these instances no complementary shift in D values, at least to any appreciable extent, is seen thereby indicating that these geothermal fluids are dominantly of meteoric origin. No  $\delta\text{D}$  data were obtained for these veins due to a lack of suitable material. Hydrogen isotope analyses provide data which allow a more definitive statement of fluid origins to be made, since D/H ratios of the fluid in a hydrothermal system will be only slightly affected, in general, by exchange with the host rock due to a paucity of primary hydrous phases (Ohmoto, 1986).

The  $^{18}\text{O}$  shift is considered to be due to the interaction of meteoric fluids which are initially isotopically light with reservoir rocks that are relatively enriched in  $^{18}\text{O}$  (Taylor, 1979; Kerrick, 1987; etc.). The water/rock ratio of a system is an important factor in determining the magnitude of the  $^{18}\text{O}$  shift, i.e., relatively low w/r ratios produce greater shifts (Ohmoto, 1986). This is due to the fact that oxygen makes up nearly 50% of most crustal rocks (Kerrick, 1987) meaning that these rocks intrinsically possess a large capacity for influencing the  $\delta^{18}\text{O}$  isotopic compositions of interstitial fluids. The process of deep circulation and exchange of meteoric waters in geothermal areas has been extended by analogy to many types of hydrothermal ore deposits (Taylor, 1974; Bethke, 1984). In addition, Walton (1987) has postulated a deep circulation model

for the Venus Vein system of Montana Mountain, immediately to the south of the Wheaton River district. Nesbitt *et al.* (1986) have stated that both epithermal and mesothermal types of deposits in the Canadian Cordillera for which they have data were formed from  $^{18}\text{O}$  evolved meteoric fluids, the mesothermal fluids experiencing deeper circulation and concomitantly greater isotopic exchange than epithermal fluids. Therefore, the hypothesis that the mineralizing fluids which deposited the galena-bearing veins in the Wheaton River district were derived from meteoric waters does not seem unreasonable. This is especially true in light of the fact that the district is situated between the Skukum and Montana Mountain deposits; both of which are considered to have been formed by meteoric waters. It is acknowledged that without further data this hypothesis lacks certainty.

#### Magmatic Derivation

Another plausible explanation which would account for the high  $\delta^{18}\text{O}_{\text{H}_2\text{O}}$  values seen would be a parent fluid which contained a high proportion of primary magmatic water which possesses a  $\delta^{18}\text{O}_{\text{H}_2\text{O}}$  range of  $\approx +5.5$  to  $+9.0\%$  (Sheppard, 1986). Primary magmatic water could have been derived from one or both of the magmatic systems which were responsible for the Skukum Volcanic Complex and the Bennett Lake Cauldron Complex. Deposition of vein material from fluids with varying primary magmatic water contents has been postulated for a number of base-precious metal vein deposits, i.e., Casapalca, Peru (Rye and Sawkins, 1974); Sunnyside, CO (Casadevall and Ohmoto, 1977); and Creede, CO (Hayba, et al., 1985) among others.

#### Metamorphic Derivation

Yet another possibility is that metamorphic fluids made up a considerable portion of the parent fluid. Metamorphic fluids would have been generated during the accretion of Terranes I and II (Monger *et al.*, 1979) from mid-Jurassic to early Tertiary. There is a great deal of uncertainty associated with the calculation of the isotopic composition of 'ideal' metamorphic fluids due to the extreme variability which is possible in the protolith



and its pre-metamorphic history (Ohmoto, 1986). Metamorphic fluids have been invoked as the principal ore-forming fluid in only a few instances; most pertinent to this discussion is probably the Mother Lode type deposits (B. F. Taylor, 1987).

#### Low $\delta^{18}\text{O}$ Galena-bearing Veins

The  $\delta^{18}\text{O}_{\text{H}_2\text{O}}$  values derived from the Mt. Anderson and Tally-Ho Hill samples seem to indicate that additional factors were influencing the deposition of these veins as compared to the system (or systems) which deposited the other galena-bearing veins. As was stated earlier, the  $\delta^{18}\text{O}_{\text{H}_2\text{O}}$  values for the Tally-Ho Hill samples are highly speculative, but the values for samples from Mt. Anderson are considered to be more reliable. As can be seen, the  $\delta^{18}\text{O}_{\text{H}_2\text{O}}$  of MAS is  $\approx 3\%$  lower than the next lowest galena-bearing vein sample (GH1) and nearly 5% lower the average for this type vein. Only the highest inferred temperature (310°C) produces a  $\delta^{18}\text{O}_{\text{H}_2\text{O}}$  value for TH4, that is not negative (0.0‰); in all probability, the true value is lower than this. Chalcedony, which gives  $\delta^{18}\text{O}_{\text{H}_2\text{O}}$  values (-15‰ to -19‰) that are very close to the assumed value for pristine meteoric water no matter which formation temperature is chosen, is found at both localities. Although the exact spatial and physical relationship of the chalcedony relative to the coarse-grained quartz is unclear in both cases, it seems more than fortuitous that the former is present in the two localities where the latter has produced the lowest  $\delta^{18}\text{O}_{\text{H}_2\text{O}}$  values.

Fluid inclusion evidence also tends to support the indication that the Mt. Anderson vein was influenced by other factors during deposition. The average Th value for the Mt. Anderson vein (226°C) is nearly 40°C below that of any other galena-bearing vein. In addition, no visible  $\text{CO}_2$  is present in this vein, while the opposite is true for every other galena-bearing vein. If, as stated before, undetected  $\text{CO}_2$  is present then salinities are the same; however, if no  $\text{CO}_2$  is present, then the Mt. Anderson vein is more saline by nearly 2wt.% NaCl.

If the chalcedony vein on Mt. Anderson was part of this low  $\delta^{18}\text{O}$  portion of the system, then the presence of fluorite in this vein may be further proof that mixing with

dilute, low temperature meteoric water took place. Richardson and Holland (1979) showed that fluorite has retrograde solubility in low salinity solutions. This means that as an initially cool meteoric fluid is warmed, fluorite will precipitate as long as NaCl concentration does not rise abruptly. Therefore, if mixing occurred gradually in the system fluorite deposition would be expected.

A mechanism which would explain the extremely low  $\delta^{18}\text{O}_{\text{H}_2\text{O}}$  values would be mixing of a near surface reservoir of isotopically light meteoric water with the more evolved waters from depth which deposited the other veins. Such a reservoir could take many forms, e.g. something as simple as a local depression in the ground water table or something as exotic as the presence of a nearby meteoric dominated epithermal system (Skukum). All that is necessary is that a large amount of meteoric water comes into contact with the ore forming fluid, whatever the nature of the reservoir. Such a mechanism, which may have been facilitated by the numerous minor faults and fractures which are present throughout the valley, would obviate the necessity of calling upon entirely separate circulation systems as an explanation for low values. These faults and fractures would have functioned as conduits for the upward migration of evolved fluids and would also have served to localize mineral deposition. Mixing of fluid types is considered to have occurred in a number of deposits; among them, the Creede district, CO (Bethke and Rye, 1979); the Finlandia vein, Peru (Kamilli and Ohmoto, 1977); and Pasto Bueno, Peru (Landis and Rye, 1974). None of these examples deals with the specific case of the presence of chalcedony or the extreme difference in  $\delta^{18}\text{O}_{\text{H}_2\text{O}}$  values; nevertheless, the documentation of fluid mixing is considered pertinent to this situation.

#### Immiscibility and Overprinting

Of the other factors which would be exerting influences to lower the  $\delta^{18}\text{O}$  values of these veins, the most likely are  $\text{CO}_2$  loss due to immiscibility and overprinting of older material by younger fluids. The effect of  $\text{CO}_2$  loss, which is due to the preferential fractionation of  $^{18}\text{O}$  to  $\text{CO}_2$  versus  $\text{H}_2\text{O}$ , is less straightforward, being dependent on both temperature and initial  $\text{CO}_2$  concentration. The findings of Kerrich (1987) indicate that

the loss of 20 mol.% CO<sub>2</sub> would result in a 3‰ depletion of the remaining fluid at a temperature of 300°C. Applying this mechanism on a district-wide scale (at least in this case) is very questionable; however, application to a particular locality may be entirely appropriate. As was discussed in Chap. V, fluid inclusion evidence suggests that the Dail Creek-Gold Hill vein system may have experienced immiscibility during its formation at approximately 300-350°C. If this is the case, the Dail Creek showing ( $\delta^{18}\text{O}_{\text{H}_2\text{O}} = +4.4\text{‰}$ ) would represent the region of the immiscibility depth, while the Gold Hill showing ( $\delta^{18}\text{O}_{\text{H}_2\text{O}} = +2.2\text{‰}$ ) would represent the depleted fluid above this depth. If the galena-bearing veins of Mt. Anderson and Tally-Ho Hill are part of the same vein system as the Dail Creek-Gold Hill system, CO<sub>2</sub> immiscibility might account for a portion of the <sup>18</sup>O depletion seen in these veins. They would, of course, represent an even higher and cooler part of the system than the Gold Hill showing. Another mechanism, such as mixing or overprinting of near-surface meteoric water with deeper fluids is still necessary to account for the low  $\delta^{18}\text{O}$  chalcedony found in these two localities.

#### **Stibnite-bearing veins**

If the stibnite-bearing veins of Carbon Hill are also part of an extended system that deposited the other vein types, then the system must have been affected by additional factors in this locality. These factors are necessary in order to account for the enriched  $\delta^{18}\text{O}_{\text{H}_2\text{O}}$  values, the lower Th values, and the CO<sub>2</sub> data. Of the sources of  $\delta^{18}\text{O}$  enriched fluids mentioned earlier (deeply circulated meteoric, magmatic, and metamorphic), the first two seem to be the most likely contributors in this case. The shear zone which hosts the vein could have served to channel either fluid type to the point of deposition. Because these veins are the most closely associated with the Tertiary volcanics of any vein type, a significant magmatic contribution is easy to imagine. However, magmatic fluids would probably also cause an increase in salinity (Ohmoto, 1986) which is not the case here. For this reason, a deeply circulated, more highly evolved meteoric fluid is the more likely contributor to these veins.

The  $\delta^{18}\text{O}_{\text{H}_2\text{O}}$  value given by sample Po15 may also be the result of the mixing of fluids on Carbon Hill, but the situation is less clear. It was noted earlier (Chap. IV) that the only sulfide found in this sample was galena; there was no stibnite, which had been identified in all other samples from this locality. In addition, this sample was taken from a small veinlet whose relationship to the principal vein in the Porter adit was unclear. The two veins appeared to be parallel, but exposures were very limited. It is possible, for lack of definite proof one way or the other, that Po15 represents an event entirely unrelated to the stibnite-bearing veins. It is possible the replacement textures so prominent in samples of the quartz from this vein indicate that overprinting of the original material by fluids from the Skukum system has occurred.

The lack of  $\delta\text{D}$  data puts a severe limit on any interpretation of the affinities of Wheaton River showings with other known deposits, but some inferences may be drawn from the  $\delta^{18}\text{O}$  and fluid inclusion data. The data suggest that the principal sulfide-bearing veins were deposited from a complex system (or systems) which was sustained either by a single fluid which underwent varying degrees of evolution due to changing physical and chemical conditions or by several fluids drawn from different sources which experienced variable degrees of mixing and evolution. Given the complex nature of the district, it is possible that the veins represent a hybrid or overlap of the mesothermal and epithermal systems described by Nesbitt, et al. (1986). That such a hybrid is possible in this area, where Tertiary felsic volcanism is in such close proximity to interplate suture zones, is unquestionable. The  $\delta^{18}\text{O}_{\text{H}_2\text{O}}$  value ranges given by these authors are -14 to -7‰ and +5 to +9‰ for epithermal and mesothermal respectively; although the ranges are not restrictive (Nesbitt, pers. comm.). Of the values seen in the present study, only those from the stibnite-bearing veins of Carbon Hill (+5.1 to +6.8) fall within either range, namely, that of the mesothermal type. All other values, except for those derived from chalcedony, lie somewhere between the two ranges with several within less than 1‰ and most within a few permil of the lower limit (+5‰) of the mesothermal type.

Walton (1987) obtained similar values for oxygen isotopes and fluid inclusion data of fluids from the mesothermal Venus vein system on Montana Mountain as those for the galena-bearing veins of this study. She felt the low  $\delta^{18}\text{O}$  value might be explained by the interaction of the fluids with a felsic volcanic host rather than the sedimentary units which host the deposits of the Nesbitt study. Felsic host rocks may also be one factor leading to the lower  $\delta^{18}\text{O}_{\text{H}_2\text{O}}$  values seen in the galena-bearing veins of this study, when compared to those of the Nesbitt study. While  $\delta^{18}\text{O}$  and fluid inclusion values from the Venus mine are very similar to those from the present study, it is acknowledged that the samples from the Wheaton River Valley are drawn from a wide area and from veins of variable mineralogy and chemistry, so that any comparisons are made with a certain amount of caution.

In summary, the ambiguity of the isotopic data and the apparent complexity of the vein systems precludes any easy explanation of vein relationships based solely on the data of this study. By invoking fluid mixing and  $\text{CO}_2$  immiscibility, it is possible to argue the conceivability of a single all-inclusive system that experienced variable degrees of both processes at different times and different localities. It is also equally possible to postulate a number of unrelated vein forming events occurring through time. As has been mentioned several times,  $\delta\text{D}$  data are necessary to make definitive statements about fluid origins. In addition, a systematic drilling program is probably needed in order to delineate various trends at depth, since data for this study was restricted to samples obtained at or near the surface in many localities.

## REFERENCES

- Angus, S., Armstrong, B., deReuck, K.M., Alumin, V.V., Gadetskii, O.G., Chapela, G.A., and Rowlinson, J.S., 1976, International thermodynamic tables of the fluid state, Vol. 3, Carbon Dioxide: Pergamon Press, Oxford, England, 385pp.
- Berger, B.R., and Eimon, P.I., 1982, Conceptual models of epithermal silver-gold deposits: AIME Preprint 82-13, 30pp.
- Bethke, P.M., 1984, Controls on base and precious metal mineralization in deeper epithermal environments: USGS Open-File Rept. 84-890, 30pp.
- Bodnar, R.J., 1983, A method of calculating fluid inclusion volumes based on vapor bubble diameters and P-V-T-X properties of inclusion fluids: Econ. Geol., v. 78, p.535-542.
- Bodnar, R.J., Burnham, C.W., and Sterner, S.M., 1985, Synthetic fluid inclusions in natural quartz. III Determination of phase equilibrium properties in the system H<sub>2</sub>O-NaCl to 1000°C and 1500 bars: Geochim. et Cosmochim. Acta, v. 49, p.1861-1873.
- Reynolds, T.J., and Kuehn, C.A., 1985, Fluid inclusion systematics in epithermal systems, *In* Geology and geochemistry of epithermal systems: Reviews in Economic Geology, Vol. 2, Soc. of Econ. Geol., p.73-98.
- Bowers, T.S., and Helgeson, H.C., 1983a, Calculation of the thermodynamic and geochemical consequences of nonideal mixing in the system H<sub>2</sub>O-CO<sub>2</sub>-NaCl on phase relations in geologic systems: Equation of state for H<sub>2</sub>O-CO<sub>2</sub>-NaCl fluids at high pressures and temperatures: Geochim. et Cosmochim. Acta, v. 47, p.1247-1275.

- and ---, 1983b, Calculation of the thermodynamic and geochemical consequences of nonideal mixing in the system  $H_2O-CO_2-NaCl$  on phase relations in geologic systems: Metamorphic equilibria at high pressures and temperatures: *Am. Mineral.*, v. 68, p.1059-1075.
- Bozzo, A.L., Chen, H.S., Kass, J.R., and Barduhn, A.J., 1975, The properties of the hydrates of chlorine and carbon dioxide: *Desalination*, v. 16, p.303-320.
- Brown, P.F., and Lamb, W.M., 1986, Mixing of  $H_2O-CO_2$  in fluid inclusions; Geobarometry and Archean gold deposits: *Geochim. et Cosmochim. Acta*, v. 50, p.847-852.
- Bull, D.R., 1986, A study of mineralogy, hydrothermal alteration, fluid inclusions and oxygen isotopes in the main quartz vein on Mount Anderson, in the Wheaton River district, southern Yukon: Unpub. B.Sc. thesis, Univ. of Alberta, 30pp.
- Burruss, R.C., 1981a, Analysis of fluid inclusions: Phase equilibria at constant volume; *Am. J. Sci.*, v. 281, p.1104-1126.
- , 1981b, Analysis of phase equilibria in C-O-H-S fluid inclusions, *in* Fluid Inclusions: Applications to Petrology: Mineral. Assoc. Can. Short Course Handbook 6, p.39-74.
- Cairnes, D.D., 1912, Wheaton district, Yukon Territory: *Geol. Sur. Can., Mem.* 31, ---, 1916, Wheaton district, southern Yukon: *Geol. Sur. Can., Sum. Rept.* 1915, p.36-49.
- Casadevall, T., and Ohmoto, H., 1977, Sunnyside Mine, Eureka Mining District, San Juan County, Colorado: Geochemistry of gold and base metal ore deposition in a volcanic environment; *Econ. Geol.*, v. 72, p.1285-1320.

- Cathles, I. M., 1977, An analysis of the cooling of intrusives by ground-water convection which includes boiling: *Econ. Geol.*, v. 72, p.804-826.
- Clayton, R.N., and Mayeda, T.K., 1963, The use of bromine pentafluoride in the extraction of oxygen from oxides and silicates for isotopic analysis: *Geochim. et Cosmochim. Acta.*, v. 27, p.43-52.
- Cockfield, W.E., and Bell, A.H., 1944, Whitehorse District, Yukon: *Geol. Sur. Can.*, Pap. 44-14, 21pp.
- Collins, P.I.F., 1979, Gas hydrates in CO<sub>2</sub>-bearing fluid inclusions and the use of freezing data for estimation of salinity: *Econ. Geol.*, v. 74, p.1435-1444.
- Craig, H., 1961, Standard for reporting concentrations of deuterium and oxygen-18 in natural waters: *Science*, v. 133, p.1833-1834.
- Crawford, M.L., 1981, Phase equilibria in aqueous fluid inclusions, *in* *Fluid Inclusions: Applications to Petrology*: Mineral. Assoc. Can., Short Course Handbook 6, p.75-100.
- Criss, R.E., and Taylor, H.P., Jr., 1986, Meteoric-hydrothermal systems, *in* *Stable isotopes in high temperature geological processes: Reviews in Mineralogy*, Vol. 16, Mineral. Soc. Amer., p.373-424.
- Cunningham, C.G., 1985, Characteristics of boiling-water-table and carbon dioxide models for epithermal gold deposition, *in* Tooke, E.W., ed., *geologic characteristics of sediment- and volcanic-hosted disseminated gold deposits--search for an occurrence model*: USGS Bull. 1646, p.43-46.



- Dagenais, G.R., 1984, The oxygen isotope geochemistry of granitoid rocks from the southern and central Yukon. Unpub. M.Sc. thesis, Univ. of Alberta, 168pp.
- and Muehlenbachs, K., 1984, Oxygen isotope contrasts between granitoid rocks of accreted and old cratonic terranes in the Yukon; GSA, Abs. with Progs., v. 16, p.482.
- Drummond, S.F., and Ohmoto, H., 1985, Chemical evolution and mineral deposition in boiling hydrothermal systems. Econ. Geol., v. 80, p.136-147.
- Elder, J.W., 1977, Model of hydrothermal ore genesis, *in* Volcanic processes in ore genesis. Inst. Mining Metall. and Geol. Soc., London, Spec. Publ. 7, p.4-13.
- Ellis, A.J., 1969, Present day hydrothermal systems and mineral deposition: Ninth Commonwealth Mining and Metallurgy Congress, Inst. of Mining and Metall. (London), p.211-240.
- Ellis, A.J., and Golding, R.M., 1963, The solubility of carbon dioxide above 100°C in water and in sodium chloride solutions: Am. J. Sci., v. 261, p.47-60.
- Field, C.W., and Fifarek, R.H., 1985, Light stable-isotope systematics in the epithermal environment, *in* Geology and geochemistry of epithermal systems: Reviews in Economic Geology, Vol. 2, Soc. of Econ. Geol., p.99-128.
- Fisher, J.R., 1976, The volumetric properties of H<sub>2</sub>O-A graphical portrayal: J. Res., USGS, v. 4, p.189-193.
- Foley, N.K., Bethke, P.M., and Rye, R.O., 1982, A re-interpretation of  $\delta D_{H_2O}$  values of

inclusion fluids in quartz from shallow ore bodies. *GSA, Abs. with Progs.*, v. 14, no. 7, p.489-490.

Fournier, R.O., 1985, Silica minerals as indicators of conditions during gold deposition, *in* Looker, F.W., ed., *Geologic characteristics of sediment- and volcanic-hosted disseminated gold deposits - search for an occurrence model*: USGS, Bull. 1646, p.15-26.

Gabrielse, H., and Wheeler, J.O., 1961, Tectonic framework of southern Yukon and northwestern British Columbia. *Geol. Surv. Can., Pap.* 60-24, 37pp.

Grond, H.C., Churchill, S.E., Armstrong, R.L., Harakal, J.F., and Nixon, G.L., 1984, Late Cretaceous age of the Hutshi, Mount Nansen, and Carmacks Groups, southwestern Yukon Territory and northwestern British Columbia: *Can. J. Earth Sci.*, v.21, p.554-558.

Haas, J.L., Jr., 1970, An equation for the density of vapor-saturated NaCl-H<sub>2</sub>O solutions from 75° to 325°C. *Am. J. Sci.*, v. 269, p.489-493.

1971, The effect of salinity on the maximum thermal gradient of a hydrothermal system at hydrostatic pressure: *Econ. Geol.*, v. 66, p.940-946.

Hanor, J.S., 1980, Dissolved methane in sedimentary brines: Potential effect on the PVT properties of fluid inclusions; *Econ. Geol.*, v. 75, p.603-617.

Hayba, D.O., 1983, A compilation of fluid inclusion and stable isotope data on selected precious- and base-metal epithermal deposits: USGS Open-File Rept. 83-450, 24p.

1985, Bethke, P.M., Heald, P., and Foley, N.K., 1985, Geologic, Mineralogic, and geochemical characteristics of volcanic-hosted epithermal precious-metal deposits, *in* *Geology and*

- geochemistry of epithermal systems. Reviews in Economic Geology, Vol. 2, Soc. of Econ. Geol., p.129-168.
- Heald, P., Foley, N.K., and Hayba, D.O., 1987, Comparative anatomy of volcanic hosted epithermal deposits acid sulfate and adularia-sericite types: Econ. Geol., v. 82, p.1-26
- Hedenquist, J.W., and Henley, R.W., 1985, The importance of CO<sub>2</sub> on freezing point measurements of fluid inclusions: Evidence from active geothermal systems and implications for epithermal ore deposition: Econ. Geol., v. 80, p.1379-1406.
- Helgeson, H.C., 1970, A chemical and thermodynamic model of ore deposition in hydrothermal systems: Min. Soc. Amer. Spec. Pap. 3, p.155-186.
- Henley, R.W., and Ellis, A.J., 1983, Geothermal systems ancient and modern: A geochemical review: Earth-Science Reviews, v. 19, p.1-50.
- Higgins, N.C., and Kerrich, R., 1982, Progressive <sup>18</sup>O depletion during CO<sub>2</sub> separation from a carbon dioxide-rich hydrothermal fluid: Evidence from the Grey River tungsten deposit, Newfoundland: Can. J. Earth Sci., v. 19, p.2247-2257.
- Hollister, I.S., 1981, Information intrinsically available from fluid inclusions, *in* Fluid inclusions: Applications to Petrology: Mineral. Assoc. Can., Short Course Handbook 6, p.1-12.
- and Burruss, R.C., 1976, Phase equilibria in fluid inclusions from the Khtada Lake Metamorphic Complex: Geochim. et Cosmochim. Acta, v. 40, p.163-175.
- , Crawford, M.L., Roedder, E., Burruss, R.C., Spooner, E.T.C., and Touret, J., 1981,

Practical aspects of microthermometry, *in* Fluid inclusions: Applications to Petrology, Mineral Assoc. Can., Short Course Handbook 6, p.278-304.

Holloway, J.R., 1981, Compositions and volumes of supercritical fluids in the earth's crust, *in* Fluid inclusions: Applications to Petrology: Mineral. Assoc. Can., Short Course Handbook 6, p.13-38.

Hvilstad, J.L., 1966, Petrology and mineralogy of the Yukon Antimony stibnite deposit, Yukon Territory, Unpub. B.Sc. thesis, Univ. of British Columbia, 32pp.

Kamilli, R.J., and Ohmoto, H., 1977, Paragenesis, zoning, fluid inclusion, and isotopic studies of the Finlandia Vein, Colqui District, Central Peru: Econ. Geol., v. 72, p.950-982.

Kerrick, R., 1987, The stable isotope geochemistry of Au-Ag deposits in metamorphic rocks, *in* Stable isotope geochemistry of low temperature fluids: Mineral. Assoc. Can. Short Course Handbook 13, p.287-336.

Kyser, J.K., 1987, Equilibrium fractionation factors for stable isotopes, *in* Stable isotope geochemistry of low temperature fluids: Mineral. Assoc. Can. Short Course Handbook 13, p. 1-76

Lambert, M.B., 1974, The Bennett Cauldron Subsidence Complex, British Columbia and Yukon Territory: Geol. Surv. Can., Bull. 227, 213pp.

Landis, G.P., and Rye, R.O., 1974, Geologic, fluid inclusion, and stable isotope studies of the Pasto Bueno tungsten-basemetal ore deposit, northern Peru: Econ. Geol., v. 69, p.1025-1059.

- LeCouteur, P.C., and Tempelman-Kluit, D.J., 1976, Rb/Sr ages and a profile of initial  $Sr^{87}/Sr^{86}$  ratios for plutonic rocks across the Yukon Crystalline Terrane: *Can. J. Earth Sci.*, v. 13, p.319-330.
- Magaritz, M., and Taylor, H.P., Jr., 1976, Isotopic evidence for meteoric-hydrothermal alteration of plutonic igneous rocks in the Yakutat Bay and Skagway Areas, Alaska: *Earth and Planet. Sci. Lett.*, v. 30, p.179-190.
- Matsuhisa, Y., Goldsmith, J.R., and Clayton, R.N., 1979, Oxygen isotopic fractionation in the system quartz-albite-anorthite-water: *Geochim. et Cosmochim. Acta*, v. 43, p.1131-1140.
- McDonald, B.W.R., and Godwin, C.I., 1986, Geology of Main Zone at Mt. Skukum, Wheaton River area, southern Yukon, *in Yukon Geology, Vol. 1: Exploration and Geological Services Division, Yukon, Indian and Northern Affairs Canada*, p.6-10.
- , ---, and Stewart, E.B., 1986, Exploration geology of the Mt. Skukum epithermal gold deposit, southwestern Yukon, *in Yukon Geology, Vol. 1: Exploration and Geological Services Division, Yukon, Indian and Northern Affairs Canada*, p.11-18.
- Monger, J.W.H., Price, R.A., and Tempelman-Kluit, D.J., 1982, Tectonic accretion and the origin of the two major metamorphic and plutonic belts in the Canadian Cordillera: *Geology*, v. 10, p.70-75.
- , Souther, J.G., and Garielse, H., 1972, Evolution of the Canadian Cordillera: A plate-tectonic model: *Am. J. Sci.*, v. 272, p.577-602.

Morrison, G.W., Godwin, C.L., and Armstrong, R.L., 1979, Interpretation of isotopic ages and  $^{87}\text{Sr}/^{86}\text{Sr}$  initial ratios for plutonic rocks in the Whitehorse map area, Yukon: *Can. J. Earth Sci.*, v. 16, p.1988-1997.

Nash, J.T., 1972, Fluid inclusion studies of some gold deposits in Nevada: USGS, Prof. Pap. 800C, p.C15-C19.

Nesbitt, B.F., Murowchik, J.B., and Muchlenbachs, K., 1986, Dual origins of lode gold deposits in the Canadian Cordillera: *Geology*, v. 14, p.506-509.

Ohmoto, H., 1986, Stable isotope geochemistry of ore deposits, *in* Stable isotopes in high temperature geological processes: *Reviews in Mineralogy* Vol. 16, Mineral. Soc. Amer., p.491-560.

O'Neil, J.R., 1986, Theoretical and experimental aspects of isotopic fractionation, *in* Stable isotopes in high temperature geological processes: *Reviews in Mineralogy*, Vol. 16, Mineral. Soc. Amer., p.1-40.

---, and Silberman, M.L., 1974, Stable isotope relations in epithermal Au-Ag deposits: *Econ.Geol.*, v. 69, p.902-909.

Parry, W.T., 1986, Estimation of  $X_{\text{CO}_2}$ , P, and fluid inclusion volume from fluid inclusion temperature measurements in the system NaCl-CO<sub>2</sub>-H<sub>2</sub>O: *Econ. Geol.*, v. 81, p.1009-1013.

Pichavant, M., Ramboz, C., and Weisbrod, A., 1982, Fluid immiscibility in natural processes: Use and misuse of fluid inclusion data I. Phase equilibria analysis--A theoretical and geometrical approach: *Chem. Geol.*, v. 37, p.1-27.

- Potter, R.W., II, 1977. Pressure corrections for fluid inclusion homogenization temperatures based on the volumetric properties of the system NaCl-H<sub>2</sub>O. USGS, J. Res., v. 5, p.603,607.
- , and Brown, D.L., 1977. The volumetric properties of aqueous sodium chloride solutions from 0° to 500°C at pressures up to 2000 bars based on a regression of available data in the literature: USGS, Bull. 1421-C; 36pp.
- , and Clynne, M.A., 1978. Solubility of highly soluble salts in aqueous media-Part 1. NaCl, KCl, CaCl<sub>2</sub>, NaSO<sub>4</sub>, and K<sub>2</sub>SO<sub>4</sub> solubilities to 100°C: USGS, J. Res., v. 6, p.701-705.
- , and Haas, J.L., Jr., 1978. Models for calculating density and vapor pressure of geothermal brines: USGS, J. Res., v. 6, p.247-257.
- , Clynne, M.A., and Brown, D.L., 1977. Freezing point depression of aqueous sodium chloride solutions: Econ. Geol., v. 73, p.284-285.
- Pride, M.J., 1985. Interlayered sedimentary-volcanic sequence Mt. Skukum Volcanic Complex, *in* Yukon Exploration and Geology 1983: Geological Services Div., DIAND, Whitehorse, p.94-104.
- , 1986. Description of the Mount Skukum Volcanic Complex, southern Yukon, *in* Yukon Geology, Vol. 1: Exploration and Geological Services Division, Yukon, Indian and Northern Affairs Canada, p.148-160.
- , and Clark, G.S., 1985. An Eocene Rb-Sr isochron for rhyolite plugs, Skukum area,

Yukon Territory: *Can. J. Earth Sci.*, v. 22, p.1747-1753.

Rambor, C., Pichavant, M., and Weisbrod, A., 1982, Fluid immiscibility in natural processes: Use and misuse of fluid inclusion data II. Interpretation of fluid inclusion data in terms of immiscibility: *Chem. Geol.*, v. 37, p.29-48.

Reed, M.H., and Spycher, N., 1984, Calculation of pH and mineral equilibria in hydrothermal waters with application to geothermometry and studies of boiling and dilution: *Geochim. et Cosmochim. Acta*, v. 48, p.1479-1492.

Reynolds, T.J., and Beane, R.F., 1985, Evolution of hydrothermal fluid characteristics at the Santa Rita, New Mexico, porphyry copper deposit: *Econ. Geol.*, v. 80, p.1328-1347.

Richardson, C.K., and Holland, H.D., 1979, Fluorite deposition in hydrothermal systems: *Geochim. et Cosmochim. Acta*, v. 43, p.1327-1335.

Roedder, E., 1984, Fluid inclusions: *Reviews in Mineralogy*, Vol. 12, Mineral. Soc. Amer., 644pp.

---, and Bodnar, R.J., 1980, Geologic pressure determinations from fluid inclusion studies: *Ann. Rev. Earth Planet. Sci.*, v. 8, p.263-301.

---, and Kopp, O.C., 1975, A check on the validity of the pressure correction in inclusion geothermometry, using hydrothermally grown quartz; IMA-Papers 9th Meeting, Berlin-Regensburg 1974, Special Issue: *Fortschritte der Mineralogie*, p.431-446.

Roots, C.F., 1981, Geological setting of gold-silver veins on Montana Mountain, *in* Yukon, Geology and Exploration, 1979-1980: Geological Services Div., DIAND, Whitehorse,



p.116-122.

Sheppard, S.M.F., 1977, Identification of the origin of ore-forming solutions by the use of stable isotopes, *in* Volcanic processes in ore genesis: Geol. Soc. London Spec. Pub. 7, p.25-41.

---, 1986, Characterization and isotopic variations in natural waters, *in* Stable isotopes in high temperature geological processes: Reviews in Mineralogy, Vol. 16, Mineral. Soc. Amer., p.165-184.

Silberman, M.L., 1983, Geochronology of hydrothermal alteration and mineralization: Tertiary epithermal precious metal deposits in the Great Basin: Geothermal Research Council, Spec. Rept. 13, p.287-303.

Sillitoe, R.H., 1977, Metallic mineralization affiliated to subaerial volcanism: A review: Inst. Mining Metall. and Geol. Soc., London, Spec. Pub. 7, p.99-116.

---, and Bonham, H.F., Jr., 1984, Volcanic landforms and ore deposits: Econ. Geol., v. 79, p.1286-1298.

Smith, M.J., 1983, Petrology and geology of high level rhyolite intrusives of the Skukum area, 105 D SW, Yukon Territory, *in* Yukon Exploration and Geology 1981: Geological Services Div., DIAND, Whitehorse, p.62-73.

Sourirajan, S., and Kennedy, G.Ç., 1962, The system H<sub>2</sub>O-NaCl at elevated temperatures and pressures: Am. J. Sci., v. 260, p.115-141.

Spooner, E.T.C., 1981, Fluid inclusion studies of hydrothermal ore deposits; Fluid Inclusions:

- Applications to Petrology: Mineral. Assoc. Can. Short Course Handbook 6, p.209-240.
- Suyisaki, R., and Jensen, M.L., 1971, Oxygen isotope studies of silicate minerals with special reference to hydrothermal mineral deposits: *Geochem. J.*, v. 5, p.7-21.
- Swanenberg, H.F.C., 1979, Phase equilibria in carbonic systems, and their application to freezing studies of fluid inclusions: *Contrib. Mineral. Petrol.*, v. 68, p.303-306.
- Takenouchi, S., and Kennedy, G.C., 1964, The binary system H<sub>2</sub>O-CO<sub>2</sub> at high temperatures and pressures: *Am. J. Sci.*, v. 262, p.1055-1074.
- , and ---, 1965, Dissociation pressures of the phase CO<sub>2</sub>\*5 3/4H<sub>2</sub>O: *J. Geol.*, v. 73, p.383-390.
- , and ---, 1965b, The solubility of carbon dioxide in NaCl solutions at high temperatures and pressures: *Am. J. Sci.*, v. 263, p.445-454.
- Taylor, B.F., 1987, Stable isotope geochemistry of ore-forming fluids, *in* Stable isotope geochemistry of low temperature fluids: Mineral. Assoc. Can. Short Course Handbook 13, p.337-445.
- Taylor, H.P., 1974, The application of oxygen and hydrogen isotope studies to problems of hydrothermal alteration and ore deposition: *Econ. Geol.*, v. 69, p.843-883.
- , 1979, Oxygen and hydrogen isotope relationships in hydrothermal mineral deposits, *in* Barnes, H.L., ed., *Geochemistry of Hydrothermal Ore Deposits*, 2ed.: John Wiley & Sons, p.236-277.

- Tempelman-Kluit, D.J., 1976, The Yukon Crystalline Terrane: Enigma in the Canadian Cordillera: GSA Bull., v. 87, p.1343-1357.
- , 1979, Transported cataclasite, ophiolite and granodiorite in Yukon: Evidence of arc-continent collision: Geol. Sur. Can., Pap. 79-14, 27pp.
- , 1980, Evolution of physiography and drainage in southern Yukon: Can. J. Earth Sci., v. 17, p.1189-1203.
- , 1981, Geology and mineral deposits of southern Yukon, *in* Yukon, Geology and Exploration, 1979-1980: Geological Services Div., DIAND, Whitehorse, p.7-31.
- , and Wanless, R.K., 1975, Potassium-argon age determinations of metamorphic and plutonic rocks in the Yukon Crystalline Terrane: Can. J. Earth Sci., v. 12, p.1895-1909.
- Wakon, L., 1987, Geology and geochemistry of the Venus Au-Ag-Pb-Zn vein deposit, Yukon Territory: Unpub. M.Sc. thesis, Univ. of Alberta, 113pp.
- Wheeler, J.O., 1961, Whitehorse Map-area, Yukon Territory, 105D: Geol. Sur. Can., Mem. 312, 156pp.
- White, D.E., 1968, Environments of generation of some base-metal ore deposits: Econ. Geol., v. 63, 301-335.
- , 1974, Diverse origins of hydrothermal ore fluids: Econ. Geol., v. 69, p.954-973.
- Wilson, F.H., Smith, J.G., and Shew, N., 1985, Review of radiometric data from the Yukon Crystalline Terrane, Alaska and Yukon Territory: Can. J. Earth Sci., v. 22, p.525-537.

## Appendix I

The following abbreviations were used where appropriate in the text.

### Mineral abbreviations.

Quartz--qtz  
Barite--bar  
Calcite--cal  
Stibnite--stib  
Sphalerite--sp  
Pyrite--py  
Galena--gn  
Chalcopyrite--cp  
Potassium feldspar--ks  
Arsenopyrite--asp  
Pyrrhotite--po  
Jamesonite--james  
Chalcedony--chal  
Tetrahedrite--tet  
Gold--Au  
Fluorite--fl

### Locality abbreviations.

Carbon Hill--CH  
Porter Claims(Carbon Hill)--Po  
Goddell's Claims(Carbon Hill)--Em  
Yukon Antimony(Carbon Hill)--YA  
Mt. Anderson--MA  
Trenches on Mt. Anderson--T1,T2,etc.  
Mt. Stevens--MS  
Tally-Ho Hill--TH  
Idaho Hill--IH  
Gold Hill--GH  
Dail Creek--DC  
Mt. Reid--MR

### Abbreviations used for reporting of fluid inclusion results.

Vol%H<sub>2</sub>O--Volume percent H<sub>2</sub>O/brine in inclusion  
Vol%CO<sub>2</sub>(l)--Volume percent CO<sub>2</sub> liquid  
Vol%CO<sub>2</sub>(g)--Volume percent CO<sub>2</sub> gas  
Vol%CO<sub>2</sub>(t)--Volume percent CO<sub>2</sub> total, where gas/liquid boundary not distinguishable  
TmCO<sub>2</sub>--Melting temperature of CO<sub>2</sub> solid  
TmIce--Melting temperature of H<sub>2</sub>O/brine  
TmClath--Melting temperature of CO<sub>2</sub> clathrate  
ThCO<sub>2</sub>--Homogenization temperature of CO<sub>2</sub>  
Th--Final homogenization temperature of entire inclusion contents  
Wt%NaCl(fpd)--Weight percent equivalent NaCl based on freezing point depression of H<sub>2</sub>O/brine  
Wt%NaCl(Clath)--Weight percent equivalent NaCl based on melting temperature of CO<sub>2</sub> clathrate

## Appendix II

Fluid inclusion data.

Inc size--longest dimension of inclusion

Homog type--only noted for inclusion that homogenized other than by complete shrinkage of bubble; mf (meniscus fades), mf-e (bubble enlarges to an extent before fading), mf-s (bubble shrank)

Sample number	origin	size	shape	lab. mass	Wt. loss	Wt. gain
				gms.	gms.	gms.
Em4	prim	12.5	rect	2.6	L-V	82
	prim	11.0	irr, e	2.3	L-V	60
Em4	prim	6.0	irr	2.3	L-V	82
	prim	10.9	irr, cir	2.4	L-V	95
Em3	prim	23.0	tub	2.6	L-V	70
	prim	26.9	irr, ext	3.1	L-V	80
	prim	5.8	rect	2.5	L-V	60
YA3	prim	4.0	irr, ov	1.8	L-V	75
	prim	17.5	irr, el	2.7	L-V	55
	prim	11.0	irr	2.8	L-V	60
	prim	12.0	irr	2.8	L-V	80
	prim	5.3	irr, bl	2.5	L-V	70
	prim	10.0	irr	3.8	L-V	60
	prim	9.0	rect	2.6	L-V	60
YA3	prim	8.0	irr	2.4	L-V	80
YA4	prim	7.5	irr	2.2	L-V	80
	prim	6.0	irr	1.8	L-V	80
YA10	prim	10.1	irr, rect	2.6	L-V	80
	prim	6.0	rect	2.3	L-V	70
YA13	prim	7.4	irr, tri	2.0	L-V	65
	prim	8.9	irr	2.4	L-V	70
YA13	prim	10.3	rect	2.7	L-V	70







Sample number	origin	inc size	inc shape	bub diam	phase	Vol% H2O	Vol% CO2(l)	Vol% CO2(g)	Vol% CO2(t)	Tm:CC2	Tm:Ice	Tm	Th:CO2	Homolog type	Wt% NaCl	Wt% NaCl	Wt% Clathr.
YA18	prim	7.5	irr	2.4	L-V	85					-4.6				2.1	2	7.3
Po2	seq	15.0	irr	2.8	L-V	85					-0.7				58.9	1.2	0.0
	sec	6.0	ov	2.0	L-V	80					-0.8				57.4	1.4	0.0
P02	prim	5.1	irr, rd	1.8	L-V	85					-4.1						
	prim	10.9	irr, bl	2.6	L-V	90					-6.5						6.6
	prim	7.9	irr	4.8	L-V		50	50		-56.8			18.7				9.9
	prim	9.2	irr	2.5	L-V		65	35		-56.7			22.9				
	prim	13.0	irr	4.9	L-V		60	40		-56.7			18.7				
Po2	prim	18.0	el	7.0	L-V		65	35		-56.8			20.7				
	prim(?)	9.0	irr	4.8	L-V		60	40		-56.8			22.5				
	prim	12.3	irr, el	4.7	L-V		60	40		-56.8			21.8				
	prim	8.0	irr, ov	4.8	L-V		55	45		-56.7			24.1				
	prim(?)	cluster			L-V					-56.7			23.1				
	prim	6.9	irr	6.9	L-V		55	45		-56.9			21.7				
	prim	4.8	irr, ov	4.8	L-V		60	40		-56.9			17.4				
Po2	prim	8.5	irr	2.6	L-V	85					-5.0				201.4	7.9	
	prim	5.5	irr, rd	2.3	L-V	80					-5.1				225.4	8.0	
	prim	9.0	irr	2.6	L-V	85					-4.8				214.8	7.5	
	sec(?)	11.5	irr	3.0	L-V	70	5	25		-57.2		7.6	28.0		277.5	0.0	4.7
P02	prim	12.1	rect	5.0	L-V	75					-4.7				176.3	7.4	
	prim	8.0	irr	5.0	L-V		45	55		-57.2			27.2	mf			
P015	prim	15.0	irr	2.8	L-V	80					-0.6				190.5	1.0	
	prim	10.0	irr, el	2.5	L-V	60					-1.0				206.1	1.7	
	prim	7.3	ov	2.4	L-V	75					-0.6				172.3	1.0	

Sample number	origin	inc size	inc shape	inc	bub diam	phase	Vol% H <sub>2</sub> O	Vol% CO <sub>2</sub> (l)	Vol% CO <sub>2</sub> (g)	Vol% CO <sub>2</sub> (t)	TmCO <sub>2</sub>	TmCO <sub>2</sub> m	TmCO <sub>2</sub> m	type	NaCl	NaC	NaC
Pot5	prim	8.2	irr		2.5	L-V	60								224.3	5.1	
	prim	6.0	rect		2.3	L-V	75								171.9	1.2	
	prim	5.0	rect		2.3	L-V	60								208.4	2.2	
	prim	7.2	ov		2.4	L-V	60								190.6	1.2	
Pot15	prim	13.0	irr		4.0	L-V	70								187.7	1.2	
	prim	13.4	irr		5.1	L-V	65								178.1	1.0	
	prim	8.6	cir		2.6	L-V	65								217.2	10.1	
	prim	11.0	irr		2.8	L-V	70								215.0	11.0	
	prim	18.0	irr, rect		2.8	L-V	80								150.9	1.4	
	prim	9.8	irr, el		2.5	L-V	70								189.9	1.0	
	prim	7.0	irr, rect		2.7	L-V	60								200.2	1.0	
Pot15	prim	6.0	bl		2.3	L-V	75								215.6	7.4	
	prim	7.1	irr, bl		2.4	L-V	80								210.1	7.7	
	prim	6.5	rd		2.1	L-V	65								204.1	8.0	
	prim	7.4	irr		2.4	L-V	65								215.9	7.9	
	prim	7.5	irr, ov		4.8	L-V	60								179.5	2.2	
	prim	20.0	irr		12.0	L-V		50	50		-57.0						
	prim	7.6	hex		2.4	L-V		25	75		-57.2						
Pot15	prim	19.0	irr		4.9	L-V	70								183.5	2.1	
	prim	13.2	irr		5.2	L-V		60	40		-57.1						
	prim	14.0	el, rect		2.7	L-V	75								193.8	1.6	
	prim	9.0	irr, ov		2.4	L-V	80								207.4	1.6	
	prim	13.0	irr, el		2.6	L-V	80								211.3	1.9	
	prim	25.0	irr		7.0	L-V	80								193.6	1.4	
	prim	11.0	irr, ov		2.7	L-V	75								216.5	1.2	
GH1	prim	6.1	irr, bl		3.2	L-V	60				-56.7		8.2		265.1		3.6

Sample number	origin	inc size	inc shape	bub diam	phase assem	Vol% H2O	Vol% CO2(l)	Vol% CO2(g)	Vol% CO2(t)	TmCO2	Tmface	Tm	ThCO2	Homog type	Th	Wt%	
																NaCl (tpd)	NaCl (Clath)
GH1	prim	7.5	irr, el	2.8	L-V	75				-56.6		7.4			282.5		5.1
	prim	5.3	irr	2.3	L-V	70						7.5			285.9		4.9
GH1	prim	14.0	irr	5.2	L-V	70			30	-57.5		7.9			266.6		4.1
	prim	7.8	irr	4.0	L-V	80			20			2.4					12.8
	prim	15.2	irr, ov	7.3	L-V	50			50	-57.3		7.8		mf-s	289.6		4.3
	prim	12.6	irr	6.0	L-V	45			55	-57.3		7.9		mf-s	309.9		4.1
	prim	12.3	irr, bl	6.5	L-V	60			40	-57.5		8.1			305.7		3.8
	prim	7.6	ird	5.1	L-V	45			55			8.3			303.4		3.4
GH1	prim	7.0	irr, rect	3.2	L-V	70			30	-56.5		8.3		mf-s	281.8		3.4
	prim	6.9	irr, tri	2.8	L-V	65			35	-56.7		8.3		mf-s	280.0		3.4
	prim	9.0	irr	4.1	L-V	75			25			7.9		mf-s	279.6		4.1
	prim	7.8	irr, tri		L-V	70			30	-56.5		8.1		mf-s	282.7		3.8
	prim	5.2	irr, ov	2.6	L-V	60			40	-56.4		7.4			279.3		5.1
GH4	prim	7.2	rect	2.6	L-V	75			25	-56.8		8.3			306.7		3.4
	prim	12.5	irr	6.8	L-V	60			40	-56.8		8.5			300.8		3.0
	prim	14.0	irr, el	4.5	L-V	80			20	-56.9		8.3			295.7		3.4
	prim	12.0	irr, el	4.5	L-V	80			20	-56.8		8.1			290.7		3.8
	prim	12.0	irr	4.8	L-V	80			20	-56.9		8.2			290.5		3.6
	prim	11.0	irr	6.5	L-V	60			40	-56.8		8.4		mf	288.2		3.2
GH4	prim	7.0	sq	2.8	L-V	75			25	-56.6		8.1			290.6		3.8
	prim	7.2	sq	3.2	L-V	70			30	-56.7		8.3			291.4		3.4
	prim	6.3	irr, bl	2.7	L-V	80			20			8.0			269.5		3.9
	prim	16.0	irr	7.0	L-V	75			25	-56.7		8.3			295.8		3.4
	prim	7.4	irr	3.2	L-V	75			25	-56.6		7.7			289.3		4.5
prim	13.0	irr, tri	2.6	L-V	85			15	-56.7		7.9			279.1		4.1	

Sample number	origin	Inc size	inc shape	bub diam	phase assem	Vol% H2O	Vol% CO2 (l)	Vol% CO2 (g)	Vol% CO2 (l)	TmCO2	Tmice	Tm	ThCO2	Homog Th type	Wt% NaCl (fpd)	Wt% NaCl (Clath)
GH5	prim	15.0	irr, cir	5.0	L-V	70									270.0	
	prim	15.0	irr, rect	5.0	L-V	60									263.3	
	sec	17.0	el	3.0	L-V	75					-0.5				193.6	0.9
	sec	13.1	irr	3.5	L-V	85					-0.5				191.5	0.9
	sec	7.4	irr, ov	2.5	L-V	70					-0.4				183.1	0.7
	sec	20.0	el	3.1	L-V	80					-0.5				202.0	0.9
	sec	7.1	el	2.5	L-V	70					-0.6				243.1	1.0
GH5	prim	18.0	el	10.0	L-L-V	35	40	25		-56.5			30.7	gas	334.3	
	prim	10.2	tri	4.8	L-V	50						7.7			253.3	4.5
	sec	9.9	hex	3.0	L-V	75					-0.6				201.5	1.0
	prim	7.8	ov	2.6	L-V	60						8.0			260.6	3.9
	prim	12.3	irr, ov	7.0	L-V	75						7.8			246.1	4.3
	prim	12.0	tri	2.6	L-V	65					-2.9				276.2	4.8
	prim	6.1	irr	2.7	L-V	50					-2.9				253.7	4.8
GH5	prim	9.7	irr, ov	2.4	L-V	75						7.1			272.3	5.6
	prim	8.2	irr, ov	2.7	L-V	60						7.1			278.2	5.6
	prim	7.5	ov	2.8	L-V	60						7.7			289.1	4.5
	prim	16.0	irr	7.3	L-V	60						6.5			286.0	5.6
DC1	prim	14.0	irr	6.4	L-V	60						8.0			287.1	3.9
	prim	17.0	irr, tri	7.3	L-V	80						7.8			284.7	4.3
	prim	17.2	irr	9.5	L-V	60						8.1			286.2	3.8
	prim	10.0	irr	3.0	L-V	60					-56.8	7.7			301.4	4.5
DC1	prim	8.0	irr	2.5	L-V	45				-57.3		7.8		mf-e	304.3	4.3
	prim	11.0	irr, rect	3.2	L-V	80				-57.2		7.8		mf-e	344.0	4.3
	prim	7.0	irr	4.2	L-V	40				-56.9		8.1		mf	324.0	3.8
	prim	11.0	irr	3.8	L-V	70				-56.9		8.1			324.0	3.8

Sample number	origin	lpc size	inc shape	bub diam	phase assem	Vol% H2O	Vol% CO2(l)	Vol% CO2(g)	Vol% CO2(t)	TmCO2	Tmlce	Tm	ThCO2	Homog type	Th	Wt%	
																NaCl	(lpad) (Clath)
DC1	prim	11.1	irr	5.2	L-V	40				-56.7		8.3	29.4	mf-e	328.4		3.4
DC1	prim	6.9	bl	4.0	L-V	40		60				8.3		mf	304.2		3.4
	prim	6.0	bl	2.3	L-V	65		35				8.2			277.6		3.6
	prim	7.0	bl	2.7	L-V	70		30		-56.7		8.0		mf	326.3		3.9
	prim	7.7	rect	2.4	L-V	75		25				8.1			268.3		3.8
DC1	prim	13.1	irr, el	5.2	L-V	55			45	-56.7		7.7		mf	320.6		4.5
	prim	9.8	irr	5.2	L-V		60	40		-56.9			30.1				
	prim	12.4	irr, el	6.9	L-V	40			60	-56.7				mf	314.6		
	prim	10.2	irr, el	5.3	L-V	40			60	-56.8				mf	306.4		
	prim	8.5	irr, el	3.4	L-V	45			55					mf	327.7		
DC1	prim	12.3	irr	5.3	L-V	45			55	-56.6		7.8		mf	312.3		4.3
	prim	13.7	irr	4.9	L-V	60			40	-56.7		7.0		mf	316.6		5.8
	prim	7.8	rect	3.7	L-V	60			40	-56.8		8.0			301.8		3.9
	prim	9.2	irr, ov	4.1	L-V	50			50	-56.7		8.1		mf	307.2		3.8
	prim	6.8	irr	2.9	L-V	45			55	-56.7		7.8		mf	316.7		4.3
MA5	prim	12.8	irr	2.7	L-V	70					-4.1				255.8	6.6	
	prim	6.0	irr, bl	2.3	L-V	55					-4.1				260.0	6.6	
	prim	9.8	irr, el	2.3	L-V	70					-3.7					6.0	
	prim	11.0	irr, bl	4.7	L-V	65					-3.5				217.3	5.7	
	prim	14.0	irr	2.6	L-V	60					-2.9				219.6	4.8	
	prim	12.0	irr	3.2	L-V	65					-3.2				211.8	5.2	
MA5	prim	10.2	irr	2.8	L-V	60									222.3	6.3	
	prim	12.3	irr	4.8	L-V	75									215.9	6.6	
MA5	prim	11.3	irr, el	5.0	L-V	65									223.0	6.1	

Sample number	origin	inc size	inc shape	bub diam	phase	Vol% H2O	Vol% CO2(l)	Vol% CO2(g)	Vol% CO2(t)	TrnCO2	TrnCO2 type	TrnCO2 Homog. Type	wt% NaCl	wt% NaCl
MA5	prim	12.8	irr	5.1	L-V	65					-4.0		247.2	6.4
	prim	10.7	irr, bl	4.7	L-V	75					-3.2		211.6	5.2
	prim	10.2	irr, ov	4.9	L-V	60					-3.7		216.9	6.0
	prim	13.9	irr, el	5.6	L-V	75					-4.1		228.3	6.6
	prim	9.6	irr	4.0	L-V	60					-3.9		214.9	6.3
	prim	11.8	irr	4.2	L-V	75					-3.7		217.8	6.0
MA9	prim(?)	25.0	rd											
	prim(?)	12.4	irr, tri	12.4	L-V	85					-0.4		189.3	0.7
	prim(?)	20.0	irr	5.2	L-V	85					-0.3		187.3	0.5
	prim(?)	20.0	irr	5.8	L-V	85					-0.3		206.6	0.5
	prim(?)	20.0	irr	5.4	L-V	85					-0.3		198.3	0.5
	prim(?)	16.5	irr	6.8	L-V	85					0.4		188.0	0.7
	prim(?)	12.0	irr	4.5	L-V	75					-0.3		186.1	0.5
	prim(?)	38.0	irr	10.1	L-V	85					-0.3		191.2	0.5
MA9	prim	20.0	irr	4.9	L-V	85					-0.4		155.7	0.7
	prim	12.2	irr	2.6	L-V	80					-0.4		175.4	0.7
	prim	12.7	irr	3.1	L-V	85					-0.3		168.2	0.5
	prim	13.0	irr, el	2.3	L-V	85					-0.3		171.1	0.5
	prim	27.0	irr	5.3	L-V	90					-0.4		160.6	0.7
	prim	13.0	irr	2.4	L-V	85					-0.4		164.8	0.7
	prim	18.0	irr	4.8	L-V	90					-0.4		171.6	0.7
MA9	prim	9.8	irr	3.0	L-V	85					-0.4		188.7	0.7
	prim	14.0	irr	3.5	L-V	85					-0.3		195.2	0.5
	prim	12.2	irr, el	2.6	L-V	75					-0.4		196.7	0.7
	prim	22.0	irr	7.2	L-V	80					-0.4		205.6	0.7
MA9	prim	13.0	irr	4.8	L-V	85					-0.4		191.3	0.7
	prim	20.0	irr	7.2	L-V	85					-0.3		188.1	0.5

Sample number	origin	Inc size	inc shape	bub diam	phase	Vol% H <sub>2</sub> O	Vol% CO <sub>2</sub> (l)	Vol% CO <sub>2</sub> (g)	Vol% CO <sub>2</sub> (t)	TmCO <sub>2</sub>	Tmice	Tm	ThCO <sub>2</sub> Homog		wt% NaCl	wt% Na <sub>2</sub> CO <sub>3</sub>
													assem	type		
MA-FL	p-sec	42.0	irr, ob	12.7	L-V	85					-0.2			173.1	0.4	
	p-sec	18.1	irr, rd	5.2	L-V	90					-0.2			174.6	0.4	
	p-sec	41.0	irr, el	11.1	L-V	85					-0.2			174.9	0.4	
MS3	prim	12.5	irr, ov	4.7	L-V	80			20			8.0		243.8		3.9
	prim	10.5	irr	3.7	L-V	85			15			7.8		270.1		4.3
	prim	11.6	irr	3.9	L-V	80			20			7.3		262.5		5.2
	prim	9.2	irr, el	3.8	L-V	80			20			8.1		265.4		3.8
	prim	7.6	irr, bl	2.1	L-V	75			25			8.3		249.1		3.4
	prim	11.8	irr, el	4.3	L-V	75			25			7.7		271.8		4.5
MS9	prim	10.0	irr, ov	2.7	L-V	75			25			7.7		251.7		4.5
	prim	12.5	irr, rect	2.0	L-V	85			15			8.2		220.7		3.6
	prim	17.5	irr, el	2.5	L-V	80			20			7.9		231.1		4.1
	prim	10.1	irr, ov	2.8	L-V	70			30			8.1		283.2		3.8
MS9	prim	10.0	irr, el	3.0	L-V	85			15			8.4		309.0		3.2
	prim	11.0	irr, bl	5.0	L-V	80			20			7.9		282.5		4.1
	prim	5.2	irr, hex	1.7	L-V	80			20			7.8		298.7		4.3
MS10	prim	8.3	irr, el	2.5	L-V	75			25			7.9		253.4		4.1
	prim	10.7	irr, ov	3.1	L-V	80			20			8.2		250.6		3.6
	prim	11.4	irr	3.7	L-V	80			29			7.8		261.2		4.3
	prim	6.8	irr	2.1	L-V	75			25			7.8		248.7		4.3
	prim	7.6	irr, el	2.4	L-V	85			15			8.1		256.2		3.8
MS10	prim	7.5	irr, el	2.0	L-V	75			25			8.1		249.4		3.8
	prim	5.0	irr, rect	2.5	L-V	85			15			8.6		262.2		2.8
MS10	sec(?)	5.0	ov	1.8	L-V	80					-0.5			202.0	0.9	0.0

Sample number	origin	inc size	inc shape	* bub diam	phase	Vol% H2O	Vol% CO2(l)	Vol% CO2(g)	Vol% CO2(l)	TmCO2	Tmlce	Tm	ThCO2	Homog type	Th	Wt% NaCl	Wt% NaCl
MS10	sec(?)	12.5	neg cryst	2.7	L-V	80					-0.6				204.6		0.0
	prim	11.1	irr	2.6	L-V	75		25				8.5			250.1		3.0
MS15	prim	7.5	irr, cir	2.7	L-V	65			35	-57.2	-0.7	7.4	30.9				5.1



Sample number	origin	inc size	inc shape	bub diam	phase assem	Vol% H2O	Vol% CO2(l)	Vol% CO2(g)	Vol% CO2(l)	TmCO2	Tm	ThCO2	Homog type	Th	Wt%	
															NaCl (fpd)	NaCl (Clath)
MA9	prim	24.0 irr		8.0	L-V	85								205.0	0.5	
	prim	17.3 irr		4.9	L-V	85								194.2	0.5	
	prim	17.0 irr		4.8	L-V	85								222.5	0.7	
	prim	26.0 irr		6.8	L-V	85								180.3	0.5	
	prim	28.0 irr		7.6	L-V	85								187.1	0.5	
MA-FI	p-sec	14.0 ov		2.8	L-V	85								175.0	0.4	
	p-sec	12.7 ov		2.7	L-V	85								176.3	0.4	
	p-sec	9.0 rd		2.5	L-V	85								178.0	0.4	
	p-sec	16.0 el		4.9	L-V	85								166.7	0.5	
	p-sec	18.2 irr		4.8	L-V	85								171.2	0.4	
	p-sec	13.0 irr		4.6	L-V	80								174.4	0.5	
	p-sec	10.3 rd		4.0	L-V	80								170.5	0.4	
MA-FI	p-sec	17.0 irr, el		4.5	L-V	85								169.0	0.4	
	p-sec	8.1 irr, ob		2.6	L-V	80								169.6	0.4	
	p-sec	14.3 irr, el		2.8	L-V	85								170.0	0.4	
MA-FI	p-sec	95.0 rect		19.4	L-V	80								165.9	0.4	
	p-sec	37.0 rd		11.2	L-V	80								168.1	0.4	
	p-sec	56.0 irr, el		10.3	L-V	80								169.1	0.4	
	p-sec	18.2 irr, rd		7.1	L-V	80								168.5	0.4	
	p-sec	49.0 irr, el		8.8	L-V	80								170.1	0.5	
	p-sec	27.0 el		9.2	L-V	80								168.2	0.5	
	p-sec	21.5 bl		7.3	L-V	80								173.2	0.4	
MA-FI	p-sec	40.3 irr, bl		11.9	L-V	85								173.3	0.4	
	p-sec	33.0 irr, ov		9.8	L-V	85								169.7	0.4	
	p-sec	16.2 ov		5.3	L-V	80								174.1	0.4	
	p-sec	69.0 irr, el		10.2	L-V	85								170.4	0.5	